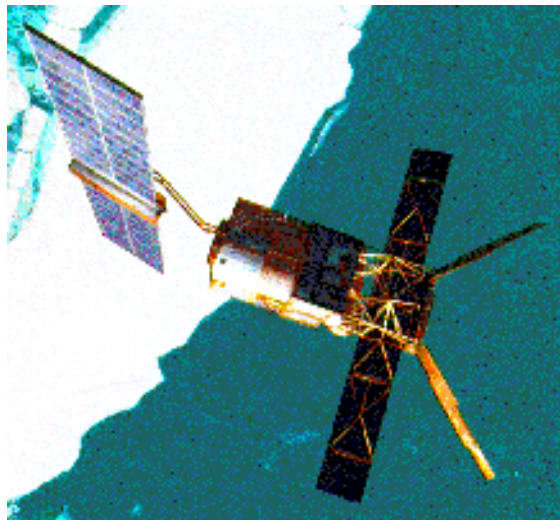


ERS-2 Wind Scatterometer Cyclic Report

from 28th February 2000 to 3rd April 2000
Cycle 51



Prepared by:

PCS team

ESRIN APP-ADQ

Inputs from:

F. Aidt
L. Isaksen

ESTEC TOS-EMS
ECMWF

Document No: APP-ADQ/PCS/WS00-004
Issue: 1.0
Date: 28th, April 2000

Distribution List

ESAHQ	G. Duchossois	
ESTEC	M. Canela E. Attema F. Aidt B. Gelsthorpe R. Zobl K. van't Klooster	APP-LR SCI-VRS TOS-EMS APP-LTP
ESOC	F. Bosquillon de Frescheville L. Stefanov	TOS-OFC TOS-OFC
ESRIN	M. Albani P. Lecomte V. Beruti S. Jutz G. Kohlhammer M. Onnestam U. Gebelein	APP-AD APP-ADQ APP-ADF APP-ADU APP-AM APP-ADC Serco
	L.A. Breivik P. Snoeij J. Heidbreder L. Isaksen J. Kerkman, J. Figa S. Pouliquen V. Wismann A. Cavanie R.S. Dunbar A. Stoffelen, T. Driessenaar G. Legg, P. Chang W. Gemmill J. Hawkins D. Offiler, R. Graham, C.A. Parrette F. Courtier, H. Roquet C. Scupniewicz R.A. Brown J. Boutin	DNMI DUT DORNIER ECMWF EUMETSAT F-PAF IFARS IFREMER JPL KNMI NOAA/NESDIS NOAA/NWS NRL UK-MET Office Meteo-France FNMOC University of Washington LODYC/UPMC

This report and its annex are also available via FTP.
ftp pooh.esrin.esa.it (login as anonymous)
cd pub/SCATTEROMETER
wscatt_rep_51.ps.Z, annex_rep_51.ps.Z

1.0 Introduction and summary

The document includes a summary of the daily quality control made within the PCS and various sections describing the results of the investigations and studying of “open-problems” related to the scatterometer, e.g. the CMOD-4 for high wind speed, the antenna pattern. In each section results are shown from the beginning of the mission in order to allow comparisons and to outline possible “seasonal” effects. An explanation of the major events that have impacted the performance since launch is given, and a comment about the recent events during the last cycle is included.

This report covers the period from 28th February 2000 to 4th April 2000 (cycle 51).

For the calibration performance the results are:

- The evolution of the maximum position of the gamma nought histograms computed over the rain forest is stable.
- The interbeam calibration shows that the fore and aft antenna signals are very close together. The difference between the fore antenna signal and the mid antenna signal is roughly 0.1 dB (both ascending and descending passes) while the difference between the aft antenna signal and the mid antenna signal seems to have a seasonal behaviour. This difference is close to 0.1 dB during the summer and it is close to 0.2 dB during the winter for the ascending passes. For the descending passes the differences between the winter and the summer is less clear and the aft-mid interbeam calibration is around 0.15 dB.
- The evolution of the sigma nought computed per relative track and for each node across the swath is stable. The time series (since December 1997 onwards) shows a high correlation among the nodes (near and far range) and the stability of the sigma nought ranges from 0.2 to 0.5 dB depending on the node. This analysis confirms the result obtained in the gamma nought monitoring.
- For cycle 51 the antenna patterns over the Brazilian rain forest (large area) are not available from ESTEC due to a hardware problem. The antenna patterns, computed by PCS over a small area of the Brazilian rain forest, for the cycle 51, are very close to the ones obtained in the previous cycle. The antenna patterns show a flat profile, within 0.3 dB for the descending passes and within 0.4dB for the ascending ones. The fore and aft antenna profiles show a small slope in the near-mid range.
- The antenna temperature monitoring over the Brazilian rain forest confirms the increase of roughly 1 degree per year for the mid and fore antenna and roughly 2 degrees per year for the aft antenna. The increase in the antennae temperature could be related with the degradation, during the years, of the antennae protection film.
- The sigma nought biases with respect to the ECMWF model first guess winds (ocean calibration) are reduced quite a bit for all three beams and all incident angles for descending tracks. For ascending tracks fore and aft beam biases are slightly smaller, compared to the result from cycle 50.
- During the cycle 51 the transponders were working nominal (apart from the passes on 21st March when they were unavailable) but no results of the calibration exercise are available yet.

For the instrument performance the results of the monitoring are:

- for the internal calibration level the power decrease during the cycle 51 was 0.09 dB. This decrease is greater than the one computed for the cycle 50 and it is due to the AMI anomalies occurred during the cycle 51 on 19th, 21st, 24th and 25th March 2000. The estimation of the power decrease over a large temporal scale is regular and it is not affected by the AMI anomalies. Since 26th October 1998 (cycle 37) the power decrease is, on average, 0.07 dB per cycle. This means that the total power decrease from cycle 37 to cycle 51 is on average 1.05 dB.
- for the Centre of Gravity (CoG) of the received spectrum the monitoring shows a regular evolution during the cycle 51. An increase of roughly 200 Hz in the CoG of the received spectrum was observed at the end of the AOCS mono-gyro qualification period (see the summary for the cycle 50). After the AOCS commissioning phase this parameter further evolved. In particular this bias was reduced by 100 Hz on 22nd March and was close to zero on the end of cycle 51. Today the CoG of the received spectrum is at the same level of the old (3 gyroes) AOCS configuration. The agreement, during one orbit, of the CoG of the received spectrum with a sinusoidal pattern is now much better in particular around 1500 seconds after the ascending node. As expected the effect of the Sun blinding (around 5500 seconds after the ascending node) is disappeared.
- for the noise power level the result is a stable evolution apart from the period 19th March - 25th March 2000 when a series of AMI anomalies caused an instability in the noise level and in the calibration level. This instability is correlated with the switch off and switch on of the AMI instrument but its origin is unknown.

For the product performance the results are:

- The AMI instrument has been operated in scatterometer mode during the ascending passes for 87.4% of the total operation time and during the descending passes for 81.5%; AMI unavailability, descoping and data lost are excluded. These values are within the nominal range.
- For cycle 51 the PCS quality control has reported stable results. The number of valid triplets acquired per day was stable around 180000 (apart from days 19th, 21th, 24th and 25th March 2000 when the number of valid triplets was less than the nominal value. This because the AMI instrument was unavailable for some orbits). The wind speed bias (UWI -ECMWF Forecast) was close to 0 m/s and the wind speed standard deviation was between 2.5 m/s and 3.0 m/s. The ambiguity removal rate was working fine for more than 90% of nodes and the wind direction is accurate for the 93% of the nodes. The ECMWF reports a wind speed bias (UWI-FG) of -0.76 m/s with a standard deviation of 1.55 m/s. The comparison between FG and 4D-var shows a wind speed bias of -0.48 with a standard deviation of 1.63 m/s. The directional bias is close to zero for both the products. The direction standard deviation is ranging between 30 and 65 degrees (UWI-FG) and between 15 and 30 degrees (FG-4D-Var). These results are very similar to the ones of the last monitoring report.

As usual the report is available via ftp (login as anonymous) to the address [pooh.esrin.esa.it](ftp://pooh.esrin.esa.it) directory /pub/SCATTEROMETER file names: [wscatt_rep_51.ps.Z](ftp://pooh.esrin.esa.it/pub/SCATTEROMETER/wscatt_rep_51.ps.Z), [annex_rep_51.ps.Z](ftp://pooh.esrin.esa.it/pub/SCATTEROMETER/annex_rep_51.ps.Z) (Unix compressed) and on the PCS web site: <http://pcswww.esrin.esa.it> (Scatterometer performance page). The statistics about the availability of the ERS-2 Wind Scatterometer raw data during cycle 51 and the detailed list of the unavailability periods are given in the document "ERS-2 AMI/RA/ATSR/GOME availability statistics" issued at the end of each cycle.

Post processed Scatterometer data acquired over tropical cyclones are available on the web site: <http://pcswww.esrin.esa.it> (cyclone tracking page).

2.0 Calibration Performances

The calibration performances are estimated using three types of target: a man made target (the transponder) and two natural targets (the rain forest and the ocean). This approach allow us to design the correct calibration using a punctual but accurate information from transponders and an extended but noisy information from rain forest and ocean for which the main component of the variance comes from the geophysical evolution of the natural target and from the backscattering models used. These aspects are in the calibration performance monitoring philosophy. The major goals of the calibration monitoring activities are the achievement of a “flat” antenna pattern profile and the assurance of a stable absolute calibration level.

2.1 Gain Constant over transponder

One gain constant is computed per transponder per beam from the actual and simulated two-dimensional echo power, which is given as a function of the orbit time and range time. This parameter clearly indicates the difference between “real instrument” and the mathematic model. In order to acquire data over the transponder the Scatterometer must be set into an appropriate operational mode that is defined as “Calibration”.

Table 1 shows the result of the calibration plan for cycle 51. The “Yes” in the EWIC column means that the raw data are available, “No” means the opposite case. The “On” in the transponder status column means that, from the raw data (EWIC), the transponders has been recognised as switched-on; “Off” means the opposite case. The “Yes” in the GC computed column means that a gain constant value has been retrieved, “No” means the opposite case.

As reported in the table no new gain constants have been computed by ESTEC.

TABLE 1. Calibration Plan: Cycle 51

DATE	ORBIT (absolute)	ORBIT (relative)	Passage	Ground Station	EWIC (raw data)	AMI mode	Transponder Status	GC computed
000229	25678	8	D	KS	Yes	Calibration	On	No
000303	25721	51	D	KS	Yes	Calibration	On	No
000318	25413	273	A	MS	Yes	Calibration	On	No
000321	25456	316	A	MS	Yes	Calibration	Off	n/a

Figure 1 and Figure 2 show the gain constants available since the beginning of the mission, the analysis is split for the different antenna elevation angle. From these figure it is clear that the gain constant measurements are stable (within +/-0.5 dB) but after the end of the commissioning phase (cycle 11) only few data are available.

The plots in Figure 3 show the value of the Gain Constant for the three beams and for the ascending, descending and all passes. The plots show the average of all gain constant available since January 1996 (cycle 8) for each antenna elevation angle. The antenna patterns are flat but there is a clear shift of the level of the curves. On average, the mid beam is 0.3 dB higher than the aft one

and 0.5 dB higher than the fore one. For the descending passes the antenna pattern shows a slight negative slope from far range to near range.

Since September 1996 ESTEC has added a scaling factor to the gain constant in order to remove the bias among the three antennae. The gain constants were increased by 0.2 dB, -0.3 dB and 0.2 dB, for the fore, mid and aft beam respectively. The result is shown in Figure 4. The suggestion given by ESTEC has not been introduced into the ground processing because the antenna patterns computed over the rain forest do not show such bias (see Figure 5). So in the actual scenario, the differences among the antennae are considered as a bias due to the transponder themselves.

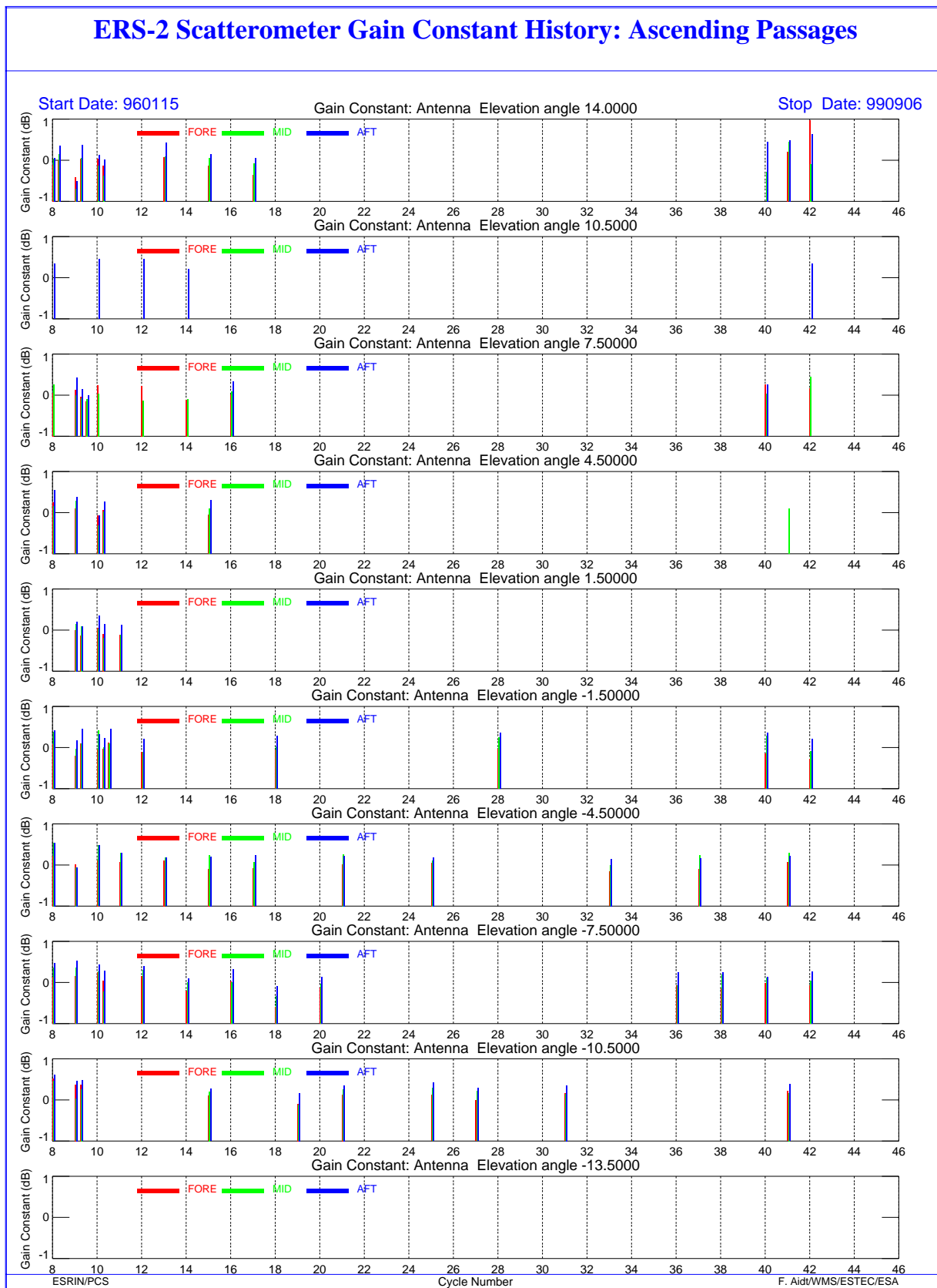


FIGURE 1. ERS-2 Scatterometer; gain Constant over transponder since the beginning of the mission (ascending passes).

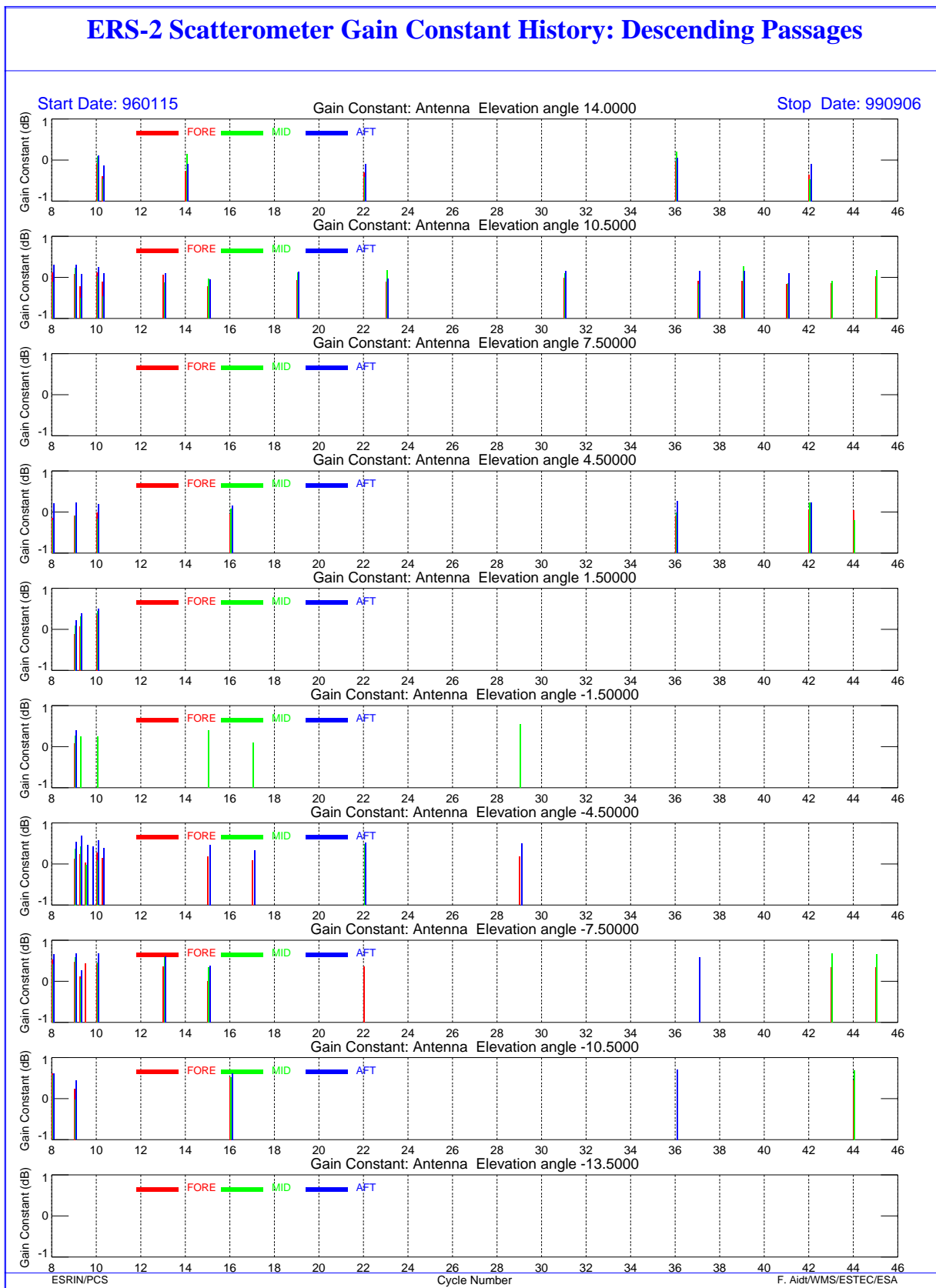


FIGURE 2. Scattermeter; gain Constant over transponder since the beginning of the mission (descending passes)

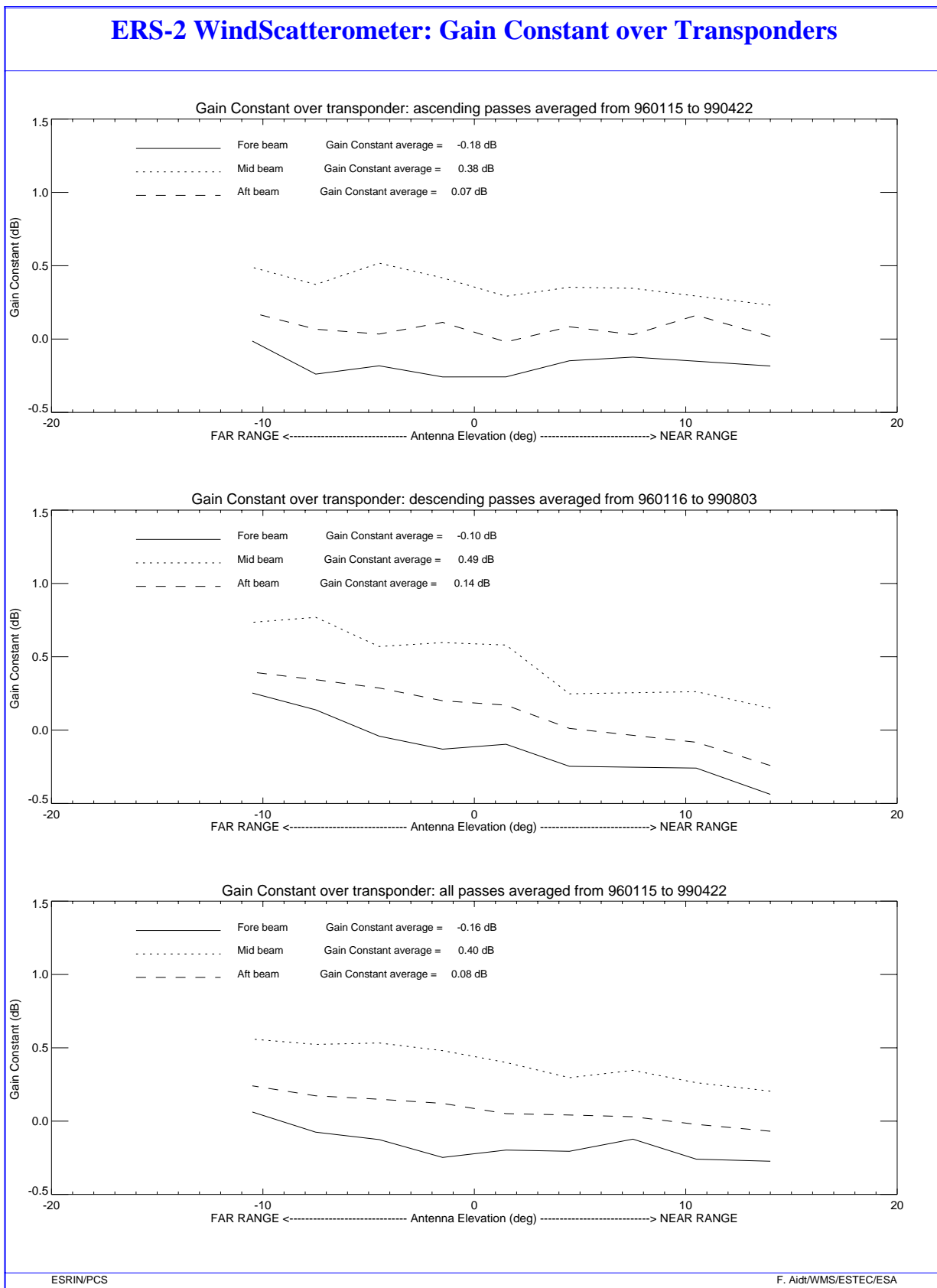


FIGURE 3. ERS-2 Scatterometer: gain constant over transponders. All data available since January 1996. Upper plot: ascending passes. Middle plot: descending passes. Lower plot: all passes.

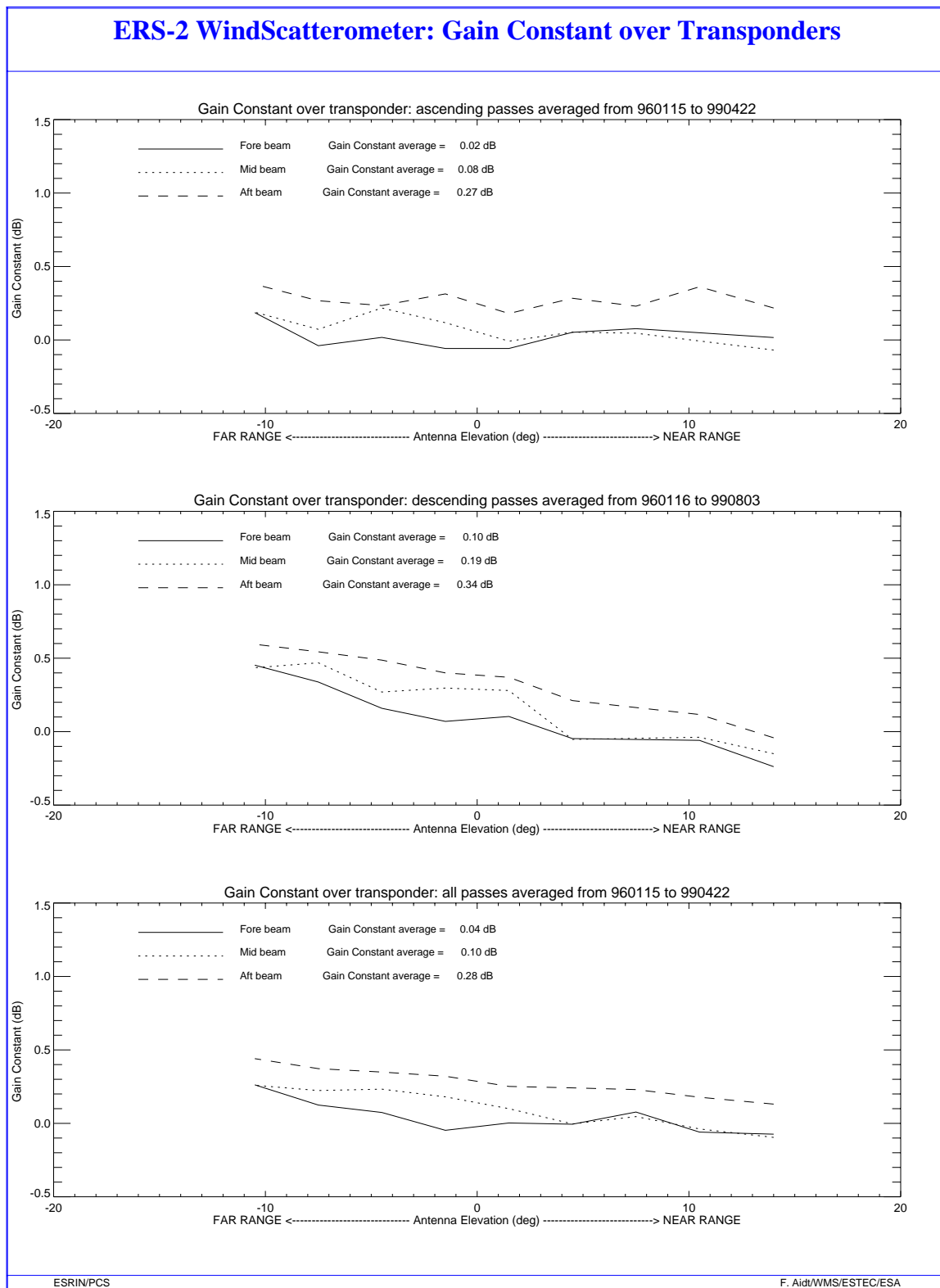


FIGURE 4. ERS-2 Scatterometer: gain constant over transponders plus a scaling factor. All data available since January 1996. Upper plot: ascending passes. Middle plot: descending passes. Lower plot: all passes.

2.2 Ocean Calibration

ECMWF performs the monitoring of ERS-2 sigma noughts over ocean (see the report in Annex).

The sigma nought bias is defined as the difference between the ERS-2 sigma-nought and the sigma nought retrieved using the CMOD-4 model with the First Guess at Appropriate Time (FGAT) background winds.

The sigma nought biases with respect to the ECMWF model first guess winds (ocean calibration) are reduced quite a bit for all three beams and all incident angles for descending tracks. For ascending tracks fore and aft beam biases are slightly smaller, compared to the result from cycle 50. The impact of the new AOCS configuration on a large scale is negligible.

2.3 Gamma-nought over Brazilian rain forest

Although the transponders give accurate measurements of the antenna attenuation at particular points of the antenna pattern, they are not adequate for fine tuning across all incidence angles, as there are simply not enough samples. The tropical rain forest in South America has been used as a reference distributed target. The target at the working frequency (C-band) of ERS-2 Scatterometer acts as a very rough surface, and the transmitted signal is equally scattered in all directions (the target is assumed to follow the isotropic approximation). Consequently, for the angle of incidence used by ERS-2 Scatterometer, the normalised backscattering coefficient (sigma-nought) will depend solely on the surface effectively seen by the instrument:

$$S^0 = S \cdot \cos \theta$$

With this hypothesis it is possible to define the following formula:

$$\gamma^0 = \frac{\sigma^0}{\cos \theta}$$

Using this relation, the gamma-nought backscattering coefficient over the rain forest is independent of the incident angle, allowing the measurements from each of the three beams to be compared.

The test area used by the PCS is located between 2.5 degrees North and 5.0 degrees South in latitude and 60.5 degrees West and 70.0 degrees West in longitude.

The following paragraphs give a description of the activities carried out with this natural target.

2.3.1 Antenna pattern: Gamma-nought as a function of elevation angle

This analysis is carried out by ESTEC that has selected a larger region than the one used as test area within PCS. In this case the selected rain forest extends from 2.0 degrees South to 11.0 degrees South in latitude and 56.0 degrees West to 80 degrees West in longitude. A large area is selected in order to have a larger amount of measurements.

For cycle 51 the antenna patterns as function of the elevation angle have not been computed by ESTEC.

2.3.2 Antenna pattern: Gamma-nought as a function of incident angle

Figure 5 shows the antenna patterns as a function of the incident angle for cycle 51.

The antenna patterns for the cycle 51 are very close to the ones obtained in the previous cycle. The antenna patterns show a flat profile, within 0.3 dB for the descending passes and within 0.4dB for the ascending ones with a small slope at the near range. The mid antenna profile is roughly 0.1 dB less than the fore and aft ones (in particular for the descending passes).

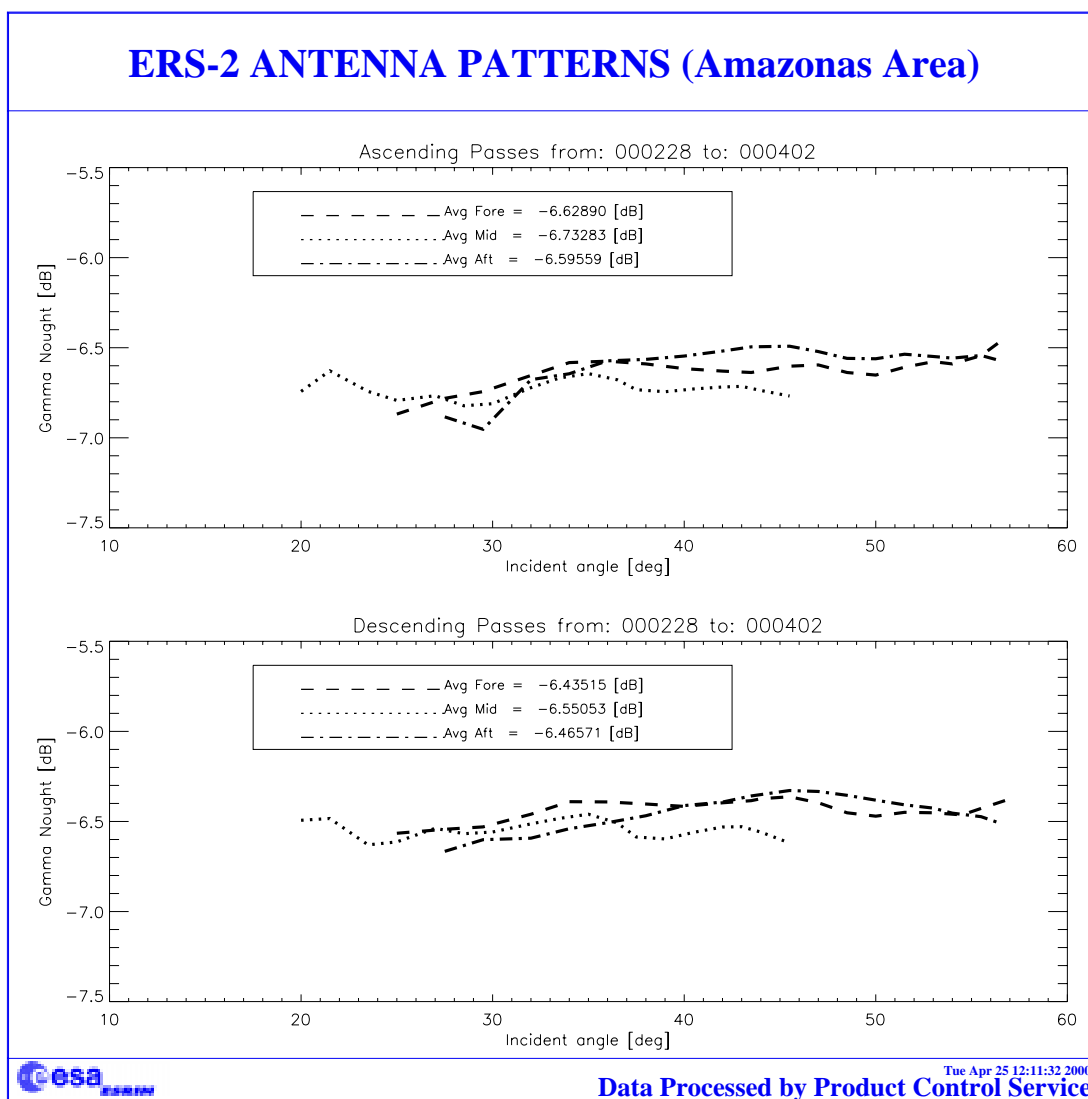


FIGURE 5. ERS-2 Scatterometer antenna patterns as function of the incident angle: cycle 51.

2.3.3 Gamma-nought histograms and peak position evolution

As the gamma-nought is independent from the incidence angle, the histogram of gamma-noughts over the rain forest is characterised by a sharp peak. The time-series of the peak position gives some information on the stability of the calibration. This parameter is computed by fitting the histogram with a normal distribution added to a second order polynomial:

$$F\langle x \rangle = A_0 \cdot \exp\left(-\frac{z^2}{2}\right) + A_3 + A_4 \cdot x + A_5 \cdot x^2$$

where:
$$z = \frac{x - A_1}{A_2}$$

The parameters are computed using a non linear least square method called “gradient expansion”. The position of the peak is given by the maximum of the function $F(x)$. The histograms are computed weekly (from Monday to Sunday) for each antenna individually (“Fore”, “Mid”, and “Aft”) and for ascending and descending passage with a bin size of 0.02 dB.

Figure 6 shows the evolution of the histograms peak position since January 1996. The step shown in March 1996 is due to the end of commissioning phase when a new Look Up Table was used in the ground stations for WSCATT FD-products generation. It is interesting to note the decrease of roughly 0.2 dB from August 1996 to June 1997. This is linked to the switch of the Scatterometer calibration subsystem from side A to side B on 6th of August. The redundancy of side A device caused a little change in the calibration that was corrected on 19th June 1997 with a new calibration LUT used in the ground processing.

Figure 7 shows the evolution of the peak position corrected with the new calibration set also for the period from August 1996 to June 1997. From the plots in figure 9 it is clear that the calibration stability achieved over the rain forest is within 0.5 dB. A seasonal effect is also present in the peak position evolution for the three antennae.

For the inter-beam calibration the results are shown in Figure 8. On average the peak values for the aft and fore antenna are very close together. The difference between the fore antenna signal and the mid antenna signal is roughly 0.1 dB (both ascending and descending passes) while the difference between the aft antenna signal and the mid antenna signal seems to have a seasonal behaviour. This differences is close to 0.1 dB during the summer and it is close to 0.2 dB during the winter for the ascending passes. For the descending passes the differences between the winter and the summer is less clear and the aft-mid inter-beam calibration is around 0.15 dB.

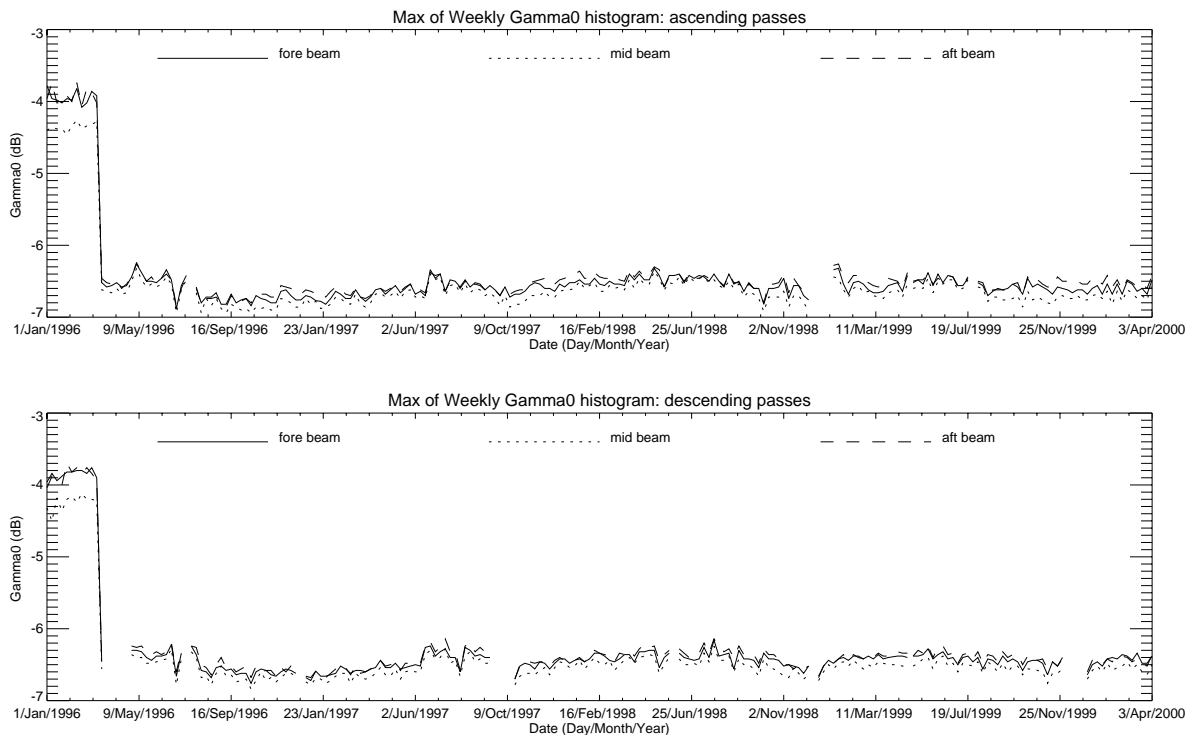


FIGURE 6. ERS-2 Scatterometer, gamma-nought histogram: weekly evolution of maximum position. From up to down: ascending passes, descending passes.

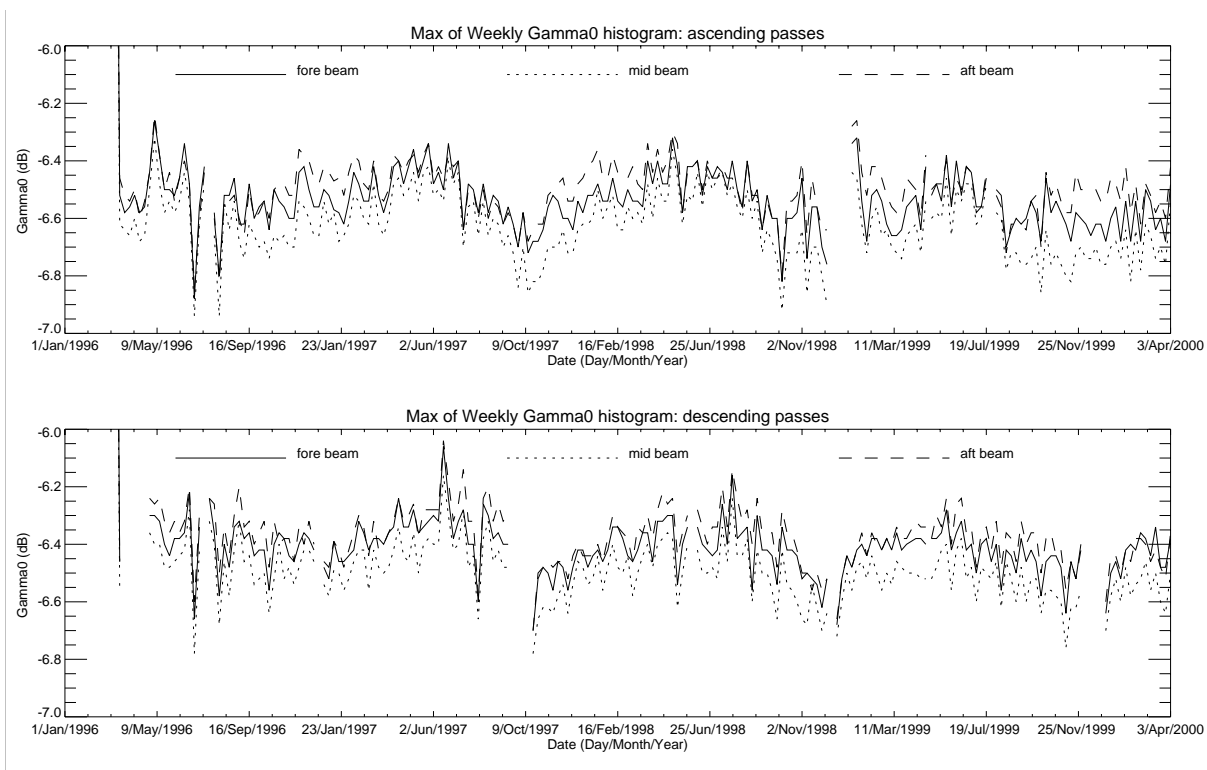


FIGURE 7. Gamma-nought histogram: weekly evolution of maximum position. Data from 6th of August 1996 to 19th June 1997 are corrected with the new calibration constant (+0.2dB). Upper plot: ascending passes. Lower plot: descending passes.

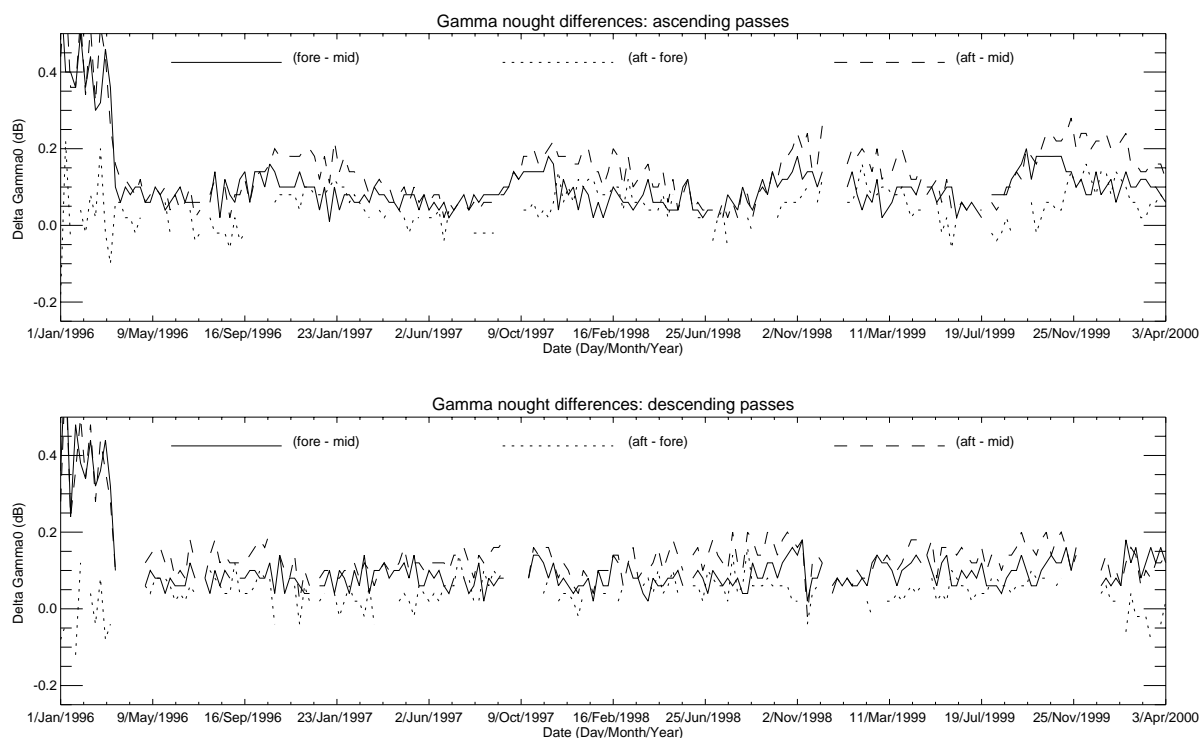


FIGURE 8. inter-beam calibration, weekly differences of the maximum position. From up to down: ascending passes, descending passes.

The mean and the standard deviation of gamma-nought are weekly computed directly using the Fast Delivery data. Figure 9 shows the evolution of the standard deviation since September 1996. The ascending passes show a gamma nought standard deviation more higher than the descending ones. This can be explained because at ascending passes the test site appears less homogeneous in particular for some areas near the rivers (see Figure 15). The last plot in Figure 11 shows the number of valid measurements used to compute the statistics. It is clear the reduction of the number of valid observation since the beginning of 1999. This is due to an increase of SAR images acquired over the Amazon rain forest.

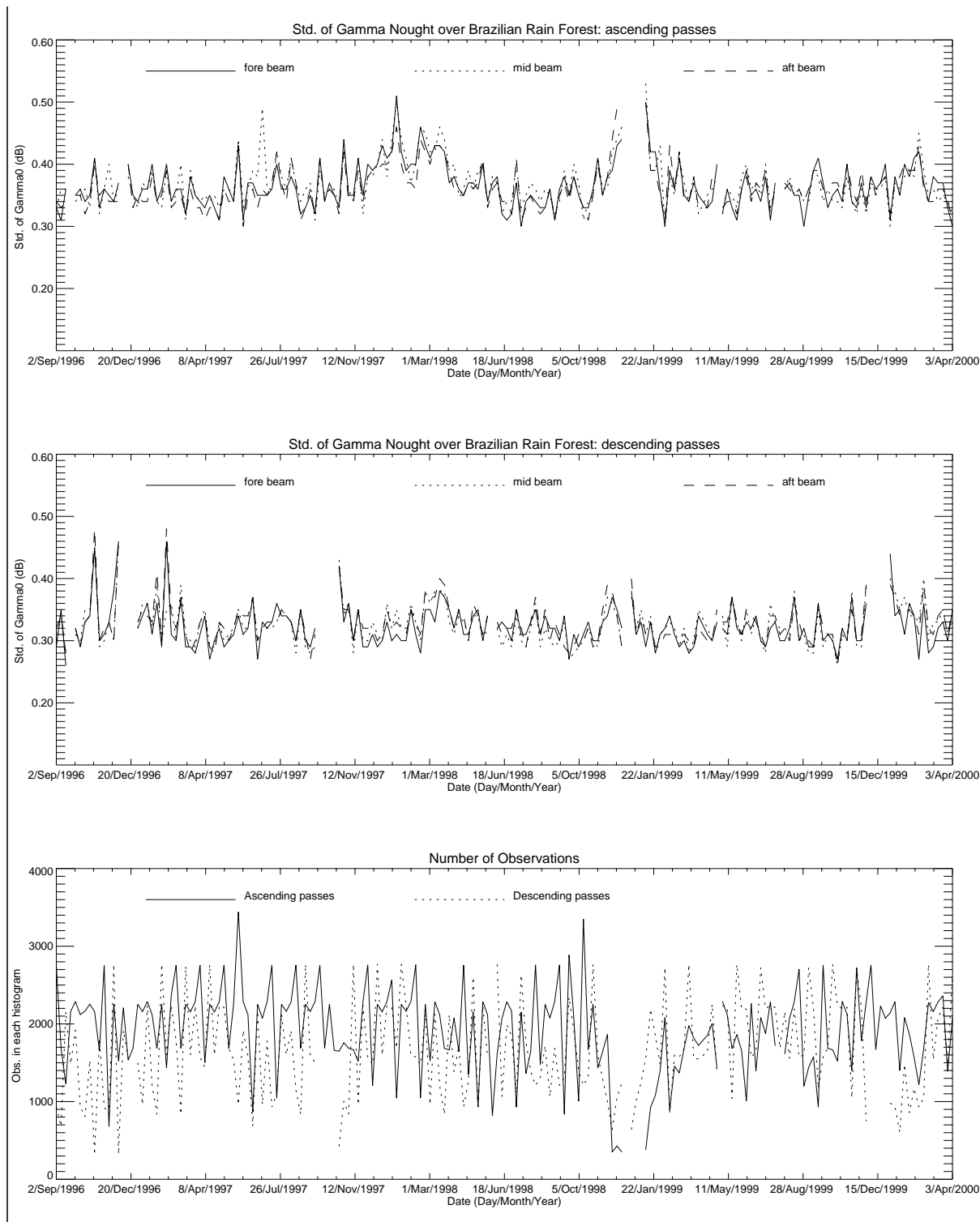


FIGURE 9. Gamma-nought histograms: weekly evolution of standard deviation. From up to down: ascending passes standard deviation, descending passes standard deviation, number of valid observations.

The Figures from 10 to 14 show the gamma-nought histogram over the Brazilian rain forest throughout cycle 51.

The shape of the weekly histograms shows slightly noise (geophysical), the position of the maximum is within the nominal range.

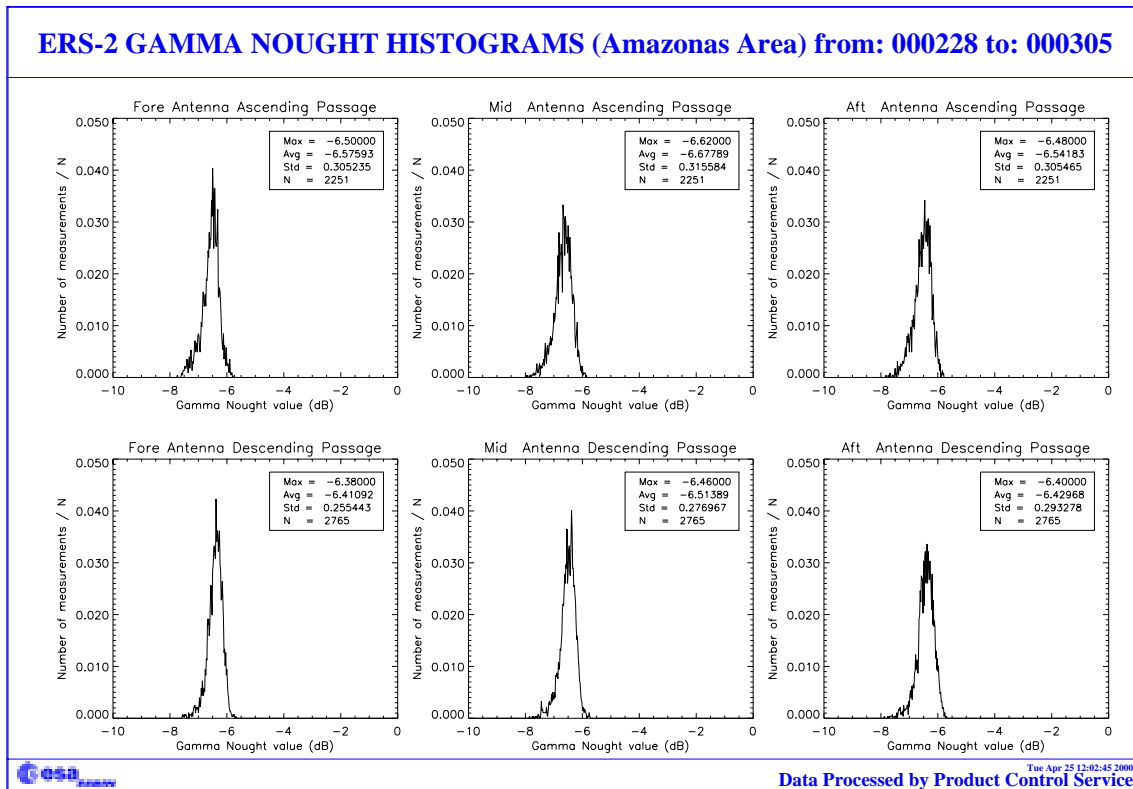


FIGURE 10. Gamma-nought histograms over Brazilian Rain forest: first week of the cycle 51

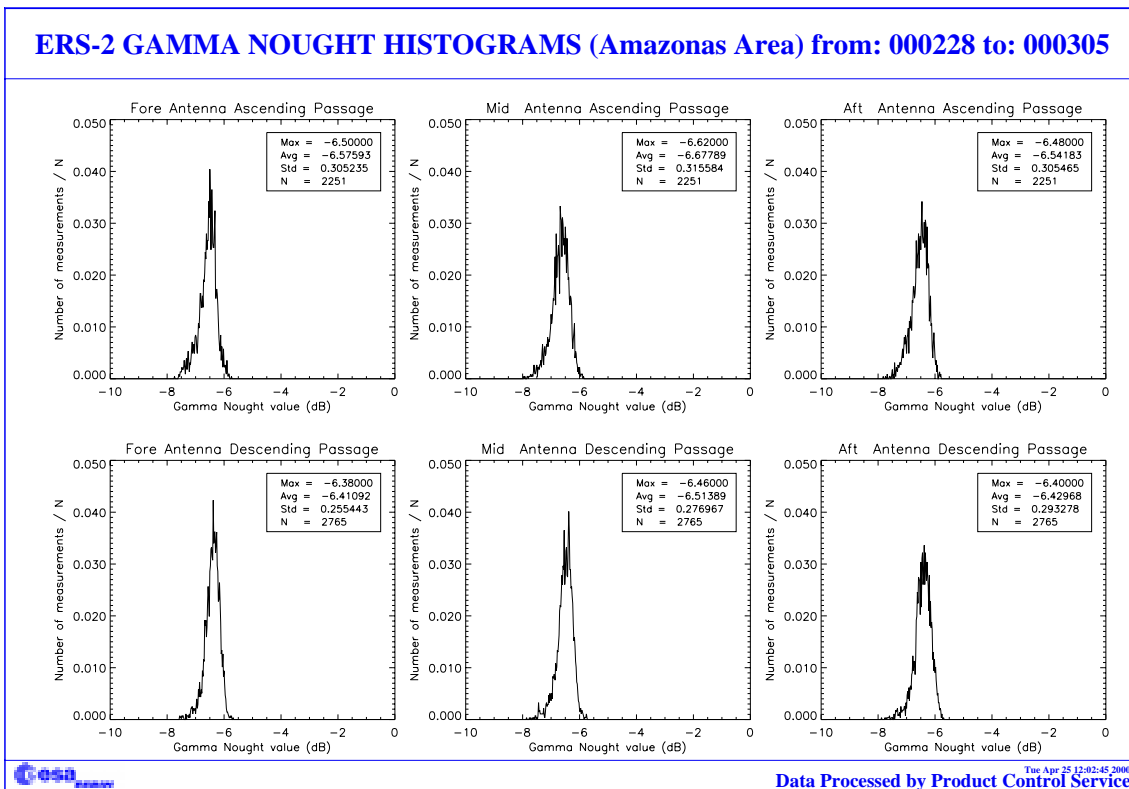


FIGURE 11. Gamma-nought histograms over Brazilian Rain forest: second week of the cycle 51

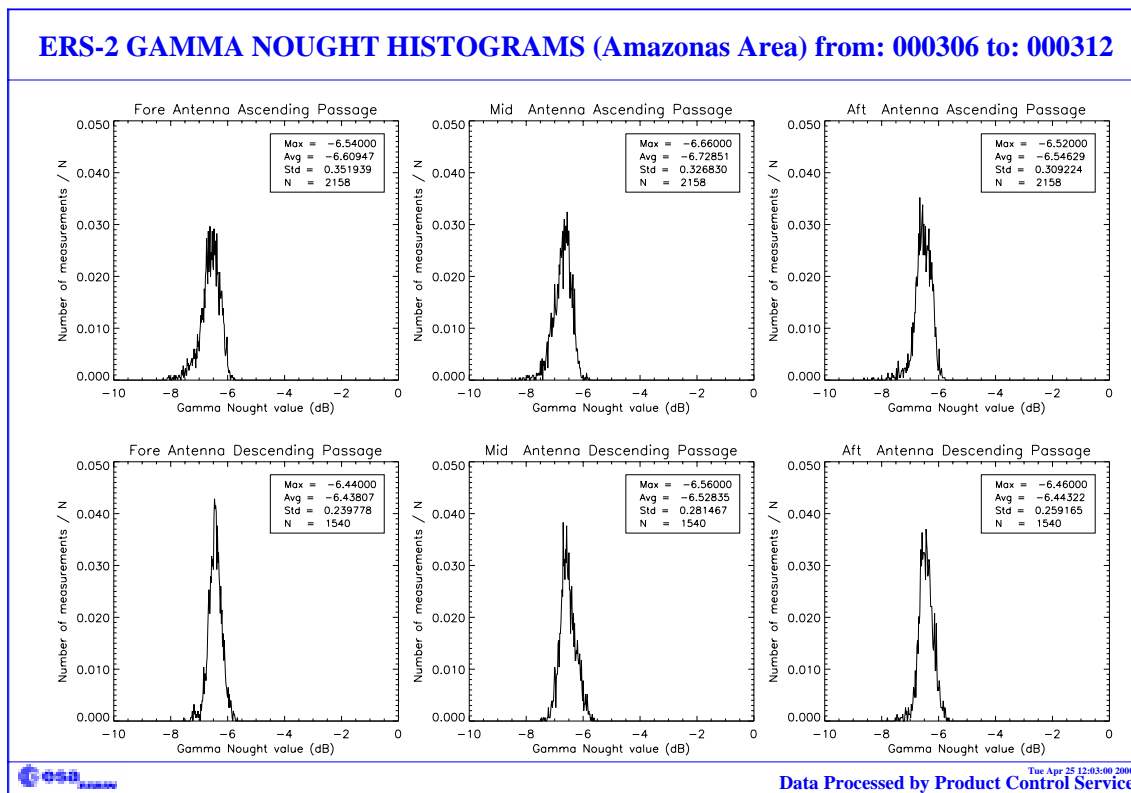


FIGURE 12. Gamma-nought histograms over Brazilian rain forest: third week of the cycle 51

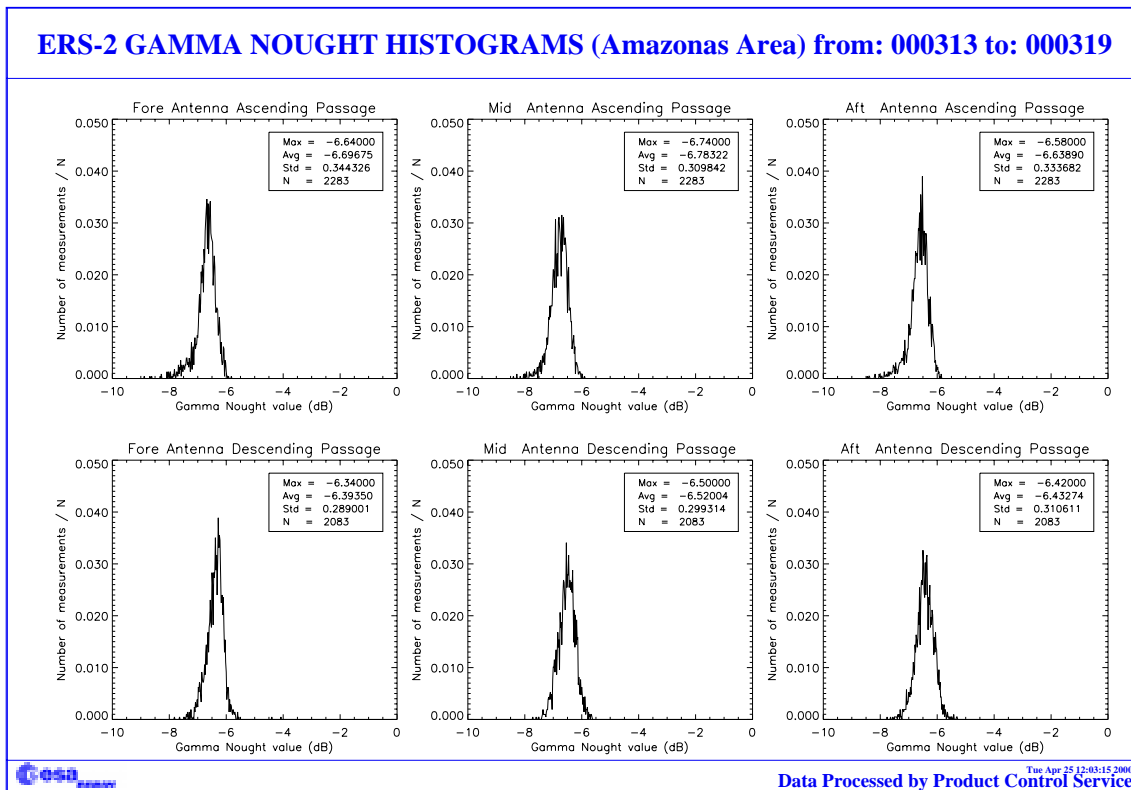


FIGURE 13. Gamma-nought histograms over Brazilian rain forest: fourth week of the cycle 51.

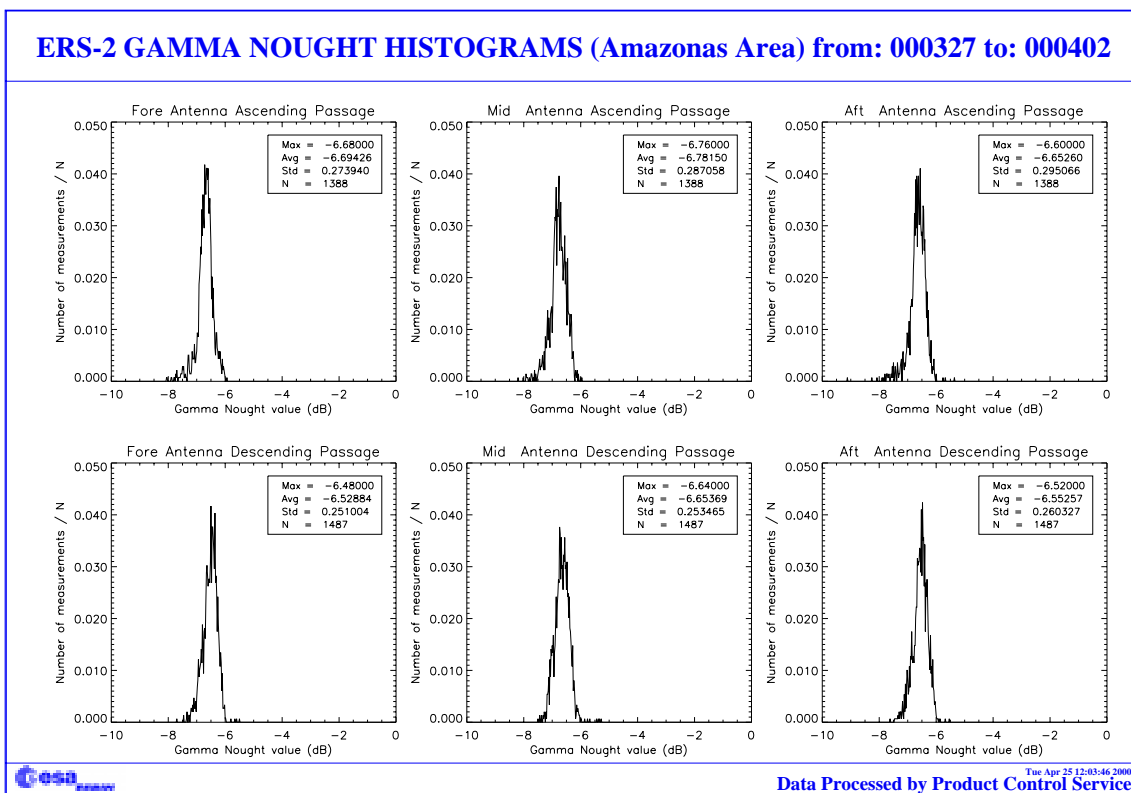


FIGURE 14. Gamma-nought histograms over Brazilian rain forest: fifth week of the cycle 51.

2.3.4 Gamma nought image of the reference area

The Figure 15 shows maps of the gamma nought over the Brazilian rain forest. This is the area where statistics are computed.

Each map has a resolution of 0.5 degrees in latitude and 0.5 degrees in longitude, roughly this is the instrument resolution at the latitude of the test site. In each resolution cell falls the average of all the valid observations available during one cycle (35 days).

From the figures no important changes happened in the test area during the cycle 51. As outlined in the previous reports the test area appears less homogenous at the ascending passes than in the descending ones. This seems due to the signal that comes from some areas near the rivers. These areas make the gamma nought histogram more noisy at ascending passes rather than at descending passes.

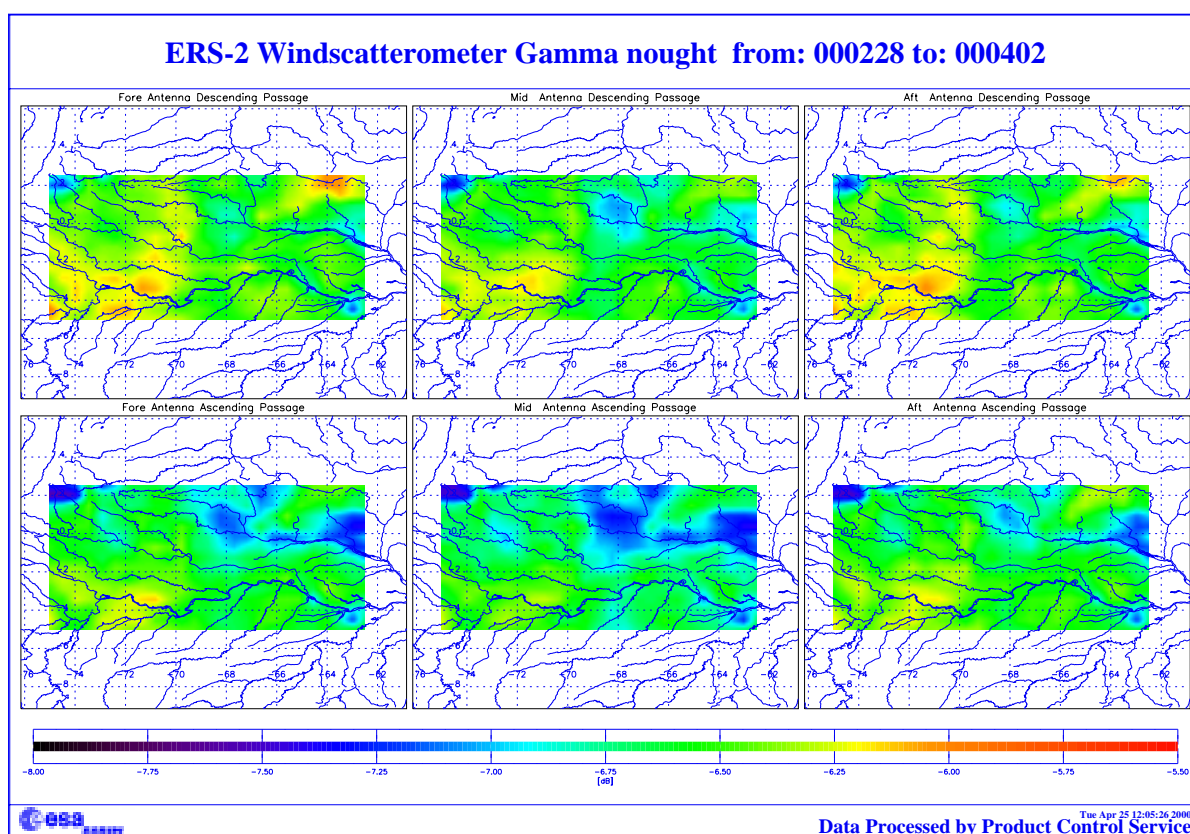


FIGURE 15. ERS-2 Scatterometer: gamma nought over the Brazilian rain forest cycle 51.

2.3.5 Sigma nought evolution

The Figures 16 and 17 show the evolution of the sigma nought (mid beam) over the reference area. The analysis is done per orbit and per node and the scope is to evaluate the stability of the sigma nought for each incident angle. The relative track chosen are those where the number of valid measurements for each node (across track) is greater than 20.

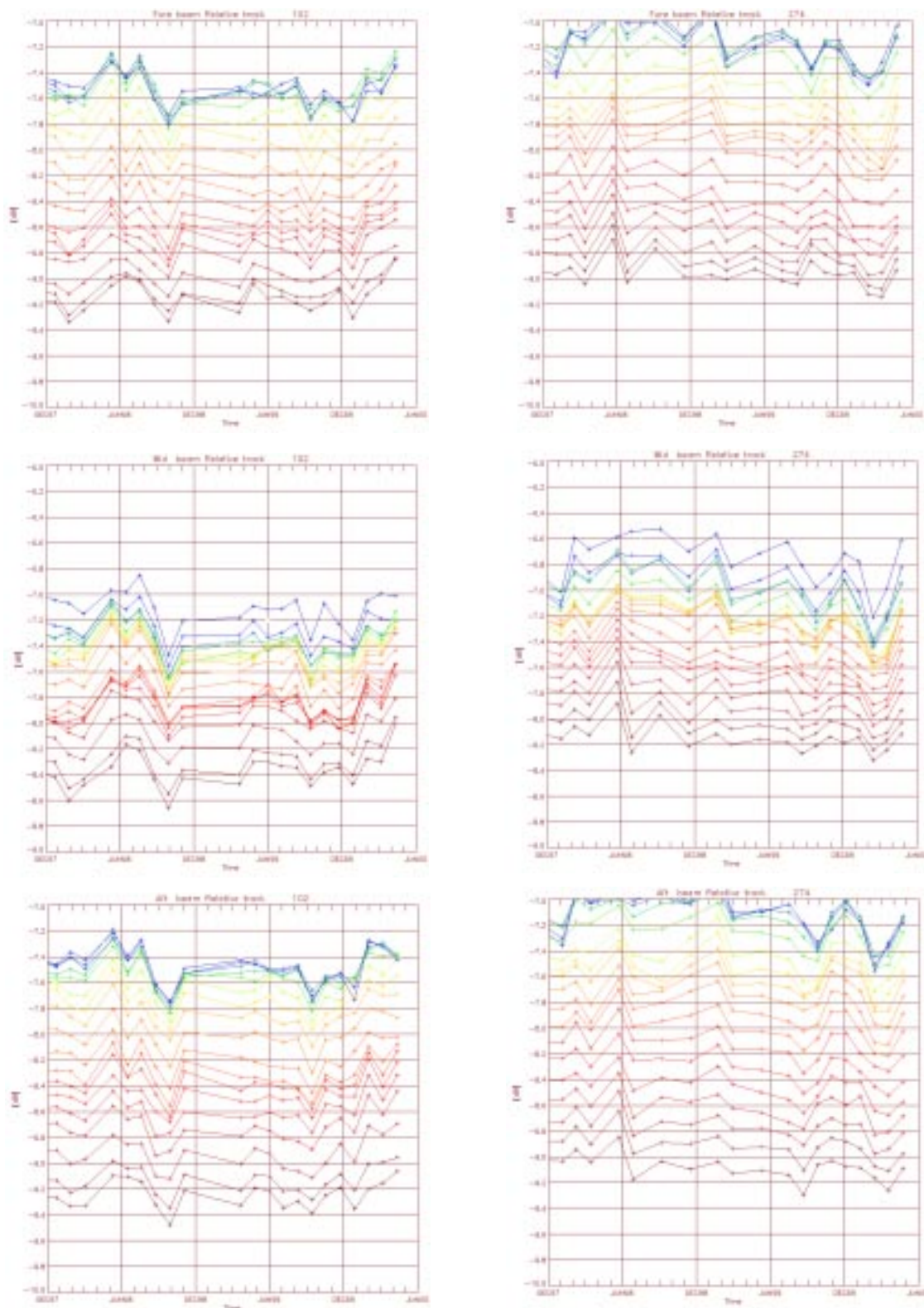


FIGURE 16. Sigma nought over the test area: ascending passes relative tracks 102 and 274; 19 nodes across the swath (since December 1997).

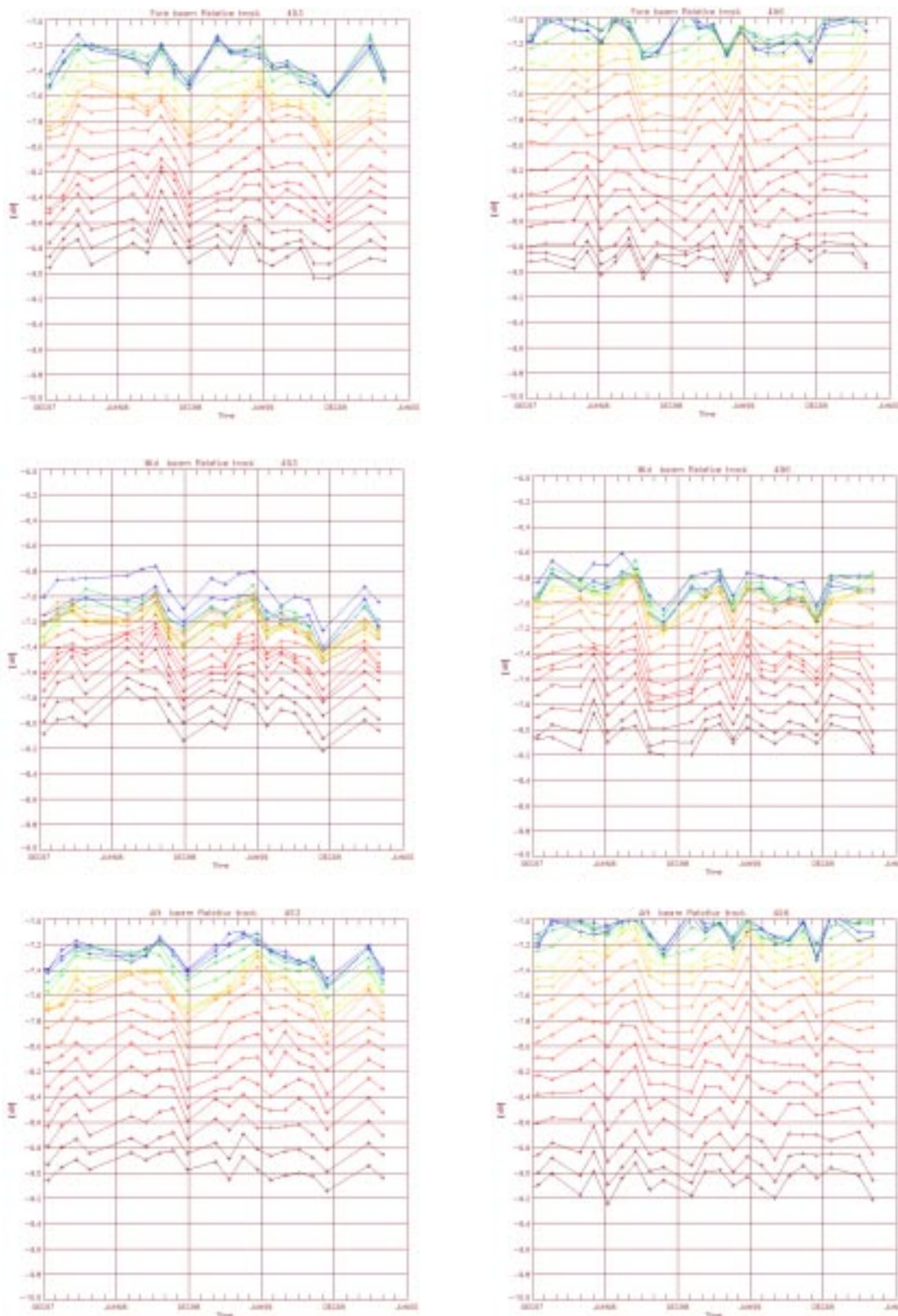


FIGURE 17. Sigma nought over the test area: descending passes relative tracks 453 and 496; 19 nodes across the swath (since December 1997).

The time series show a high correlation among the nodes (near and far range) and the stability of the sigma nought ranges from 0.2 to 0.5 dB depending on the node. This analysis confirms the result obtained in the gamma nought monitoring.

2.3.6 Antenna temperature evolution over the Rain Forest

The monitoring of the antenna temperature over the Brazilian rain forest is performed by PCS. The antenna temperatures are retrieved from the satellite telemetry when the Scatterometer swath is over the test site and the instrument is active (AMI in wind only or wind/wave mode). The scope of this monitoring is to investigate a possible correlation between the antenna temperatures and the gamma-nought level. This correlation is not clear in the actual data because of the gamma nought variability of the selected area. A deep analysis is to be performed to better understand the facts.

The plots for the three beams and for the ascending, descending and all passes are in Figure 18. It is interesting to note that the annual variation is due to the earth inclination and that the antenna temperatures have an increase of roughly 1.0 degree per year in the case of the mid and fore antenna; 2 degrees per year for the aft antenna.

This temperature increase could be related to the degradation of the antennae protection film.

ERS-2 WindScatterometer: Antennas Temperature Evolution Over Rain Forest

Data available for descending passes : 779

Data available for ascending passes : 909

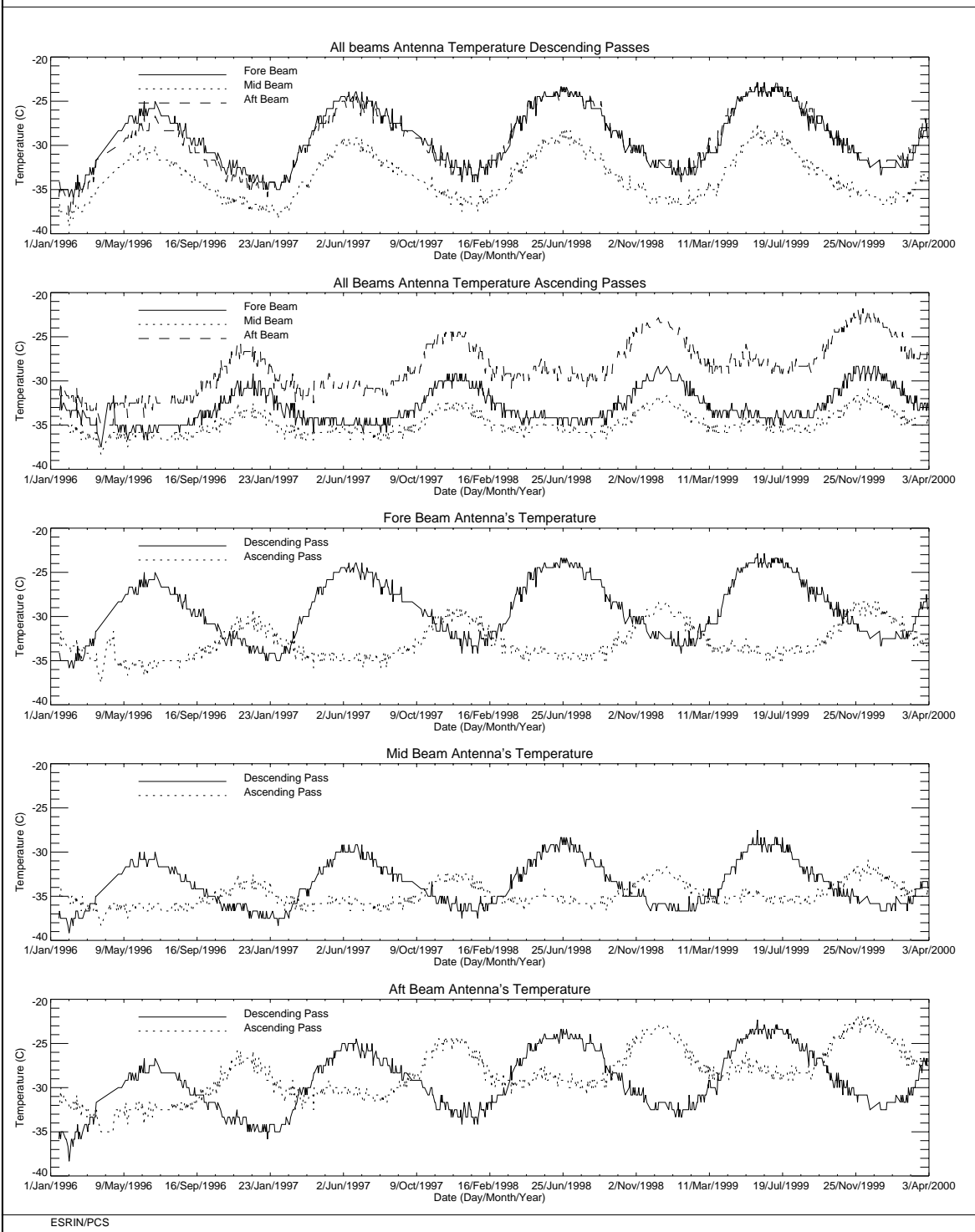


FIGURE 18. ERS-2 Scatterometer: evolution of the antenna temperatures over the Brazilian rain forest.

3.0 Instrument performance

The instrument status is checked by monitoring the following parameters:

- Centre of Gravity (CoG) and standard deviation of the received signal spectrum. This parameter is useful for the monitoring of the orbit stability, the performances of the doppler compensation filter, the behaviour of the yaw steering mode and the performances of the devices in charge for the satellite attitude (e.g. gyroscopes, earth sensor).
- Noise power I and Q channel.
- Internal calibration pulse power.

the latter is an important parameter to monitor the transmitter and receiver chain, the evolution of pulse generator, the High Power Amplifier (HPA), the Travelling Wave Tube (TWT) and the receiver.

These parameters are extracted daily from the UWI products and averaged. The evolution of each parameter is characterised by a least square line fit. The coefficients of the line fit are printed in each plot.

3.1 Centre of gravity and standard deviation of received power spectrum

The Figure 19 shows the evolution of the two parameters for each beam.

The tendency from the beginning of the mission to the operation with the new Attitude On-board Control System (AOCS) configuration (7th February 2000) is a clear and regular increase of the Centre of gravity (CoG) of received spectrum for the three antennae. An increase of roughly 200 Hz was observed at the end of the AOCS qualification period. After the AOCS commissioning phase this parameter further evolved. In particular this bias was reduced by 100 Hz on 22nd March and was close to zero on the end of cycle 51 (3rd April 2000). Today the CoG of the received spectrum is at the same level of the old (3 gyros) AOCS configuration. (see also Figure 20).

The old AOCS configuration (one Digital Earth Sensor - DES, one Digital Sun Sensor - DSS and 3 gyros) is no more considered safe because 3 of the six gyros on-board are out of order or very noisy. The new attitude control configuration is designed to pilot the ERS-2 using only one gyro plus the DES and the DSS modules. Scope of this new configuration is to extend the satellite lifetime by using the available gyros one at the time.

The evolution of the standard deviation of the CoG of the received spectrum is more stable apart from the change occurred on 26th, October 1998. On October 26th, 1998 the standard deviation of the CoG had, on average, a decrease of roughly 100 Hz for the fore and aft antenna and of roughly 30Hz for the mid antenna. This change is linked with the increase of the transmitted power (see 3.3).

Others changes in the AOCS configuration are recognised in Figure 19. The two steps observed at the beginning of the plots of the CoG (see Figure 19) are due to a change in the pointing subsystem (DES reconfiguration) side B instead of side A after a depointing anomaly (see table 2 for the list of the AOCS depointing anomaly occurred during the ERS-2 mission). The first change is

from 24th, January 1996 to 14th, March 1996, the second one is from 14th February 1997 to 22nd April 1997. During these periods side B was switched on. It is important to note that during the first time a clear difference in the CoG of the received spectrum is present only for the Fore antenna (an increase of roughly 100 Hz) while during the second time the change has affected all the three antennae (roughly an increase of 200 Hz, 50 Hz and 50 Hz for the fore, mid and aft antenna respectively).

Table 2: ERS-2 Scatterometer AOCS depointing anomaly

From	To
24 th January 1996 9:10 a.m.	26 th January 1996 6:53 p.m
14 th February 1996 1:25 a.m.	15 th February 1996 3:44 p.m
3 rd June 1998 2:43 p.m.	6 th June 1998 12:47 a.m.
1 st September 1999 8:50 a.m.	2 nd September 1999 1:28 a.m.

The Figure 19 shows also when the satellite was operated in Fine Pointing Mode (FPM) or the on-board doppler compensation was missing. These events are related with the large peaks in the CoG of the received spectrum plots (fore and aft antenna) and are listed in Table 3.

Table 3: ERS-2 Scatterometer anomalies in the CoG fore and aft antenna

Date	Reason
26 th and 27 th September 1996	missing on-board doppler coefficient (after cal. DC converter test period)
6 th and 7 th June 1998	no Yaw Steering Mode (after depointing anomaly)
2 nd and 3 rd December 1998	missing on-board doppler coefficients (after AMI anomaly 228)
16 th and 17 th February 2000	Fine Pointing Mode (FPM) (due to AOCS mono-gyro qualification period)

The peaks shown in the plot of mid beam standard deviation of the CoG of the received spectrum are linked to the satellite manoeuvres and AOCS anomaly.

Figure 21 shows the averaged CoG of the received spectrum (mid antenna) as time function from the ascending node (time = 0). Each unit of the X axis is 5 seconds from the ascending node while the Y axis is the frequency in Hz. Figure 21 is relative to the beginning of April 2000. The solid line in the plots is the retrieved (unwrapping) CoG of the received spectrum from the values stored in the UWI products (as shown in the dotted line). The effect of the sun blinding (for details see the report for the cycle 50) is disappeared as expected.

The Figure 22 compares the AOCS 3-gyro configuration CoG of the received spectrum (solid line) with the AOCS mono-gyro(5) configuration (dotted line) for two cases: during the qualification period (upper plot) and at the beginning of April 2000 (lower plot). The curves are obtained filtering the CoG of the received spectrum evolution throughout the orbit. For reference the level of the 3 gyroes case is shifted up to reach the zero doppler at the ascending node.

It is clear from the plots in Figure 22 that now the agreement of the evolution of the CoG of the received spectrum between the case of mono-gyro and three gyroes configuration is better than the one obtained during the qualification period.

ERS-2 WindScatterometer: DOPPLER COMPENSATION Evolution (UWI)

Least-square poly. fit fore beam	Center of gravity = $-307.5 + (0.1056) \cdot \text{day}$	Standard Deviation = $4241.6 + (0.0570) \cdot \text{day}$
Least-square poly. fit mid beam	Center of gravity = $-645.7 + (0.1048) \cdot \text{day}$	Standard Deviation = $5128.3 + (0.0090) \cdot \text{day}$
Least-square poly. fit aft beam	Center of gravity = $-362.4 + (0.0911) \cdot \text{day}$	Standard Deviation = $4367.5 + (0.0412) \cdot \text{day}$

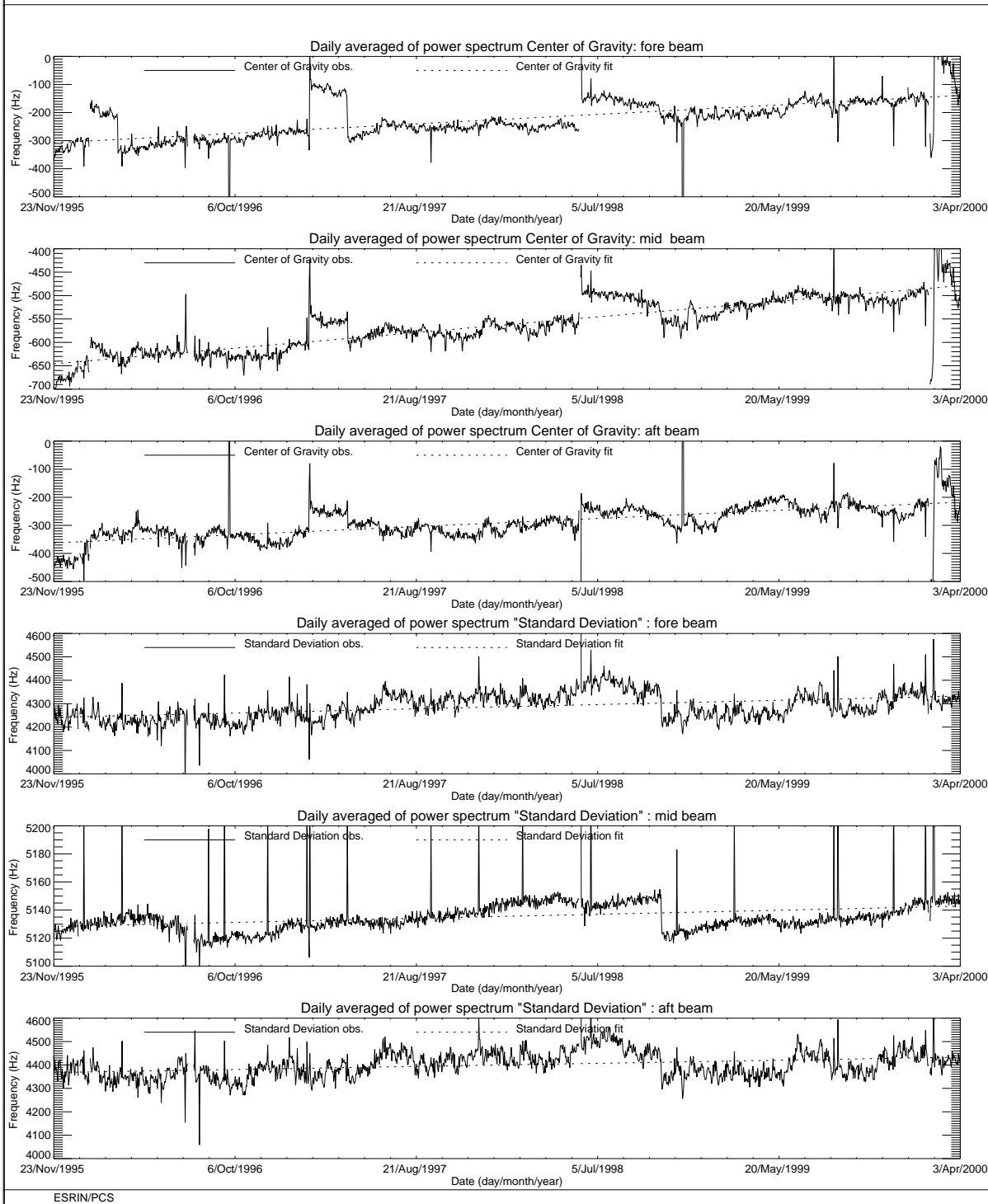


FIGURE 19. ERS-2 Scatterometer: Centre of Gravity and standard deviation of received power spectrum since the beginning of the mission.

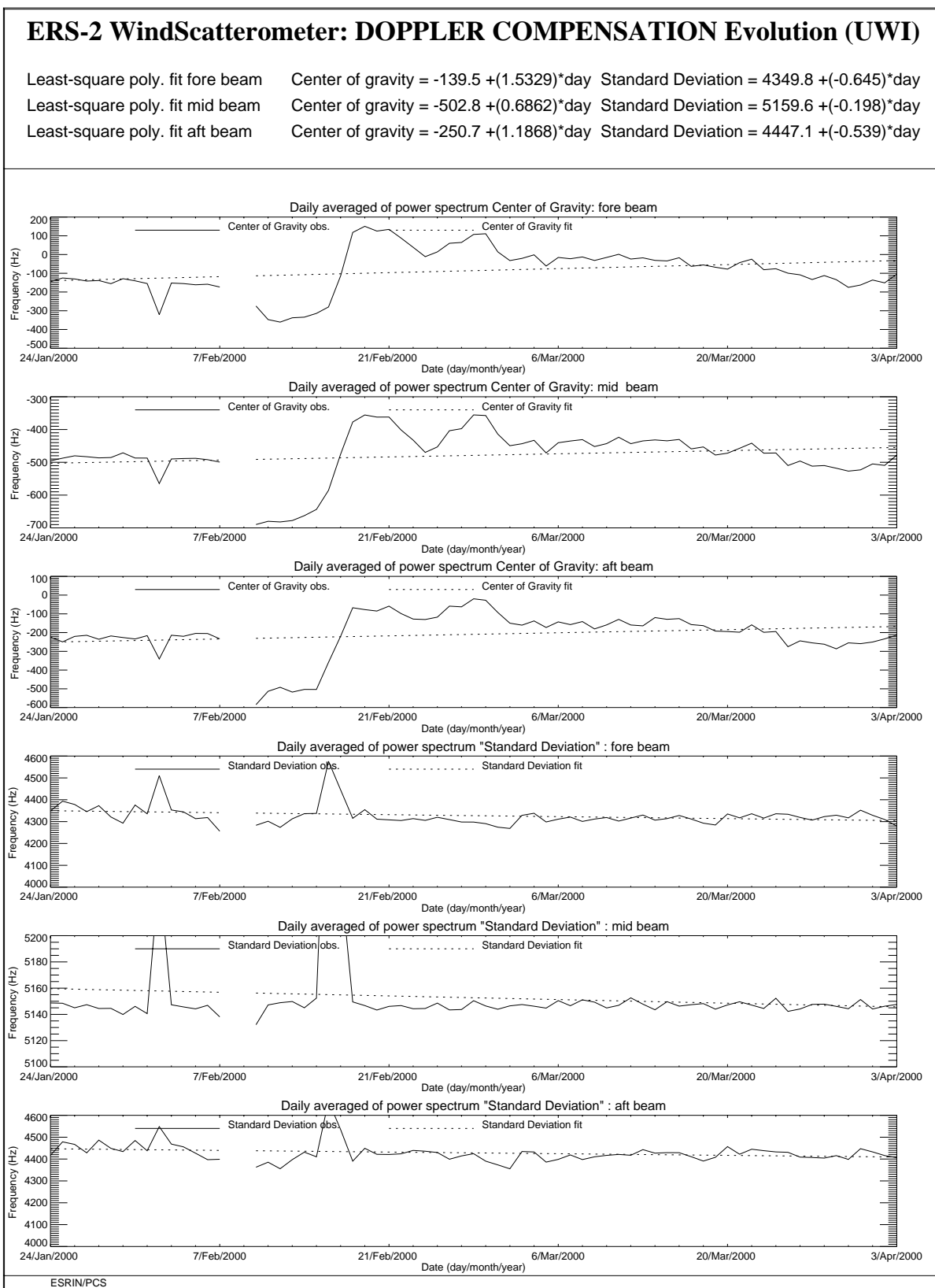


FIGURE 20. ERS-2 Scatterometer: Centre of Gravity and standard deviation of received power spectrum during the cycle 50 and cycle 51.

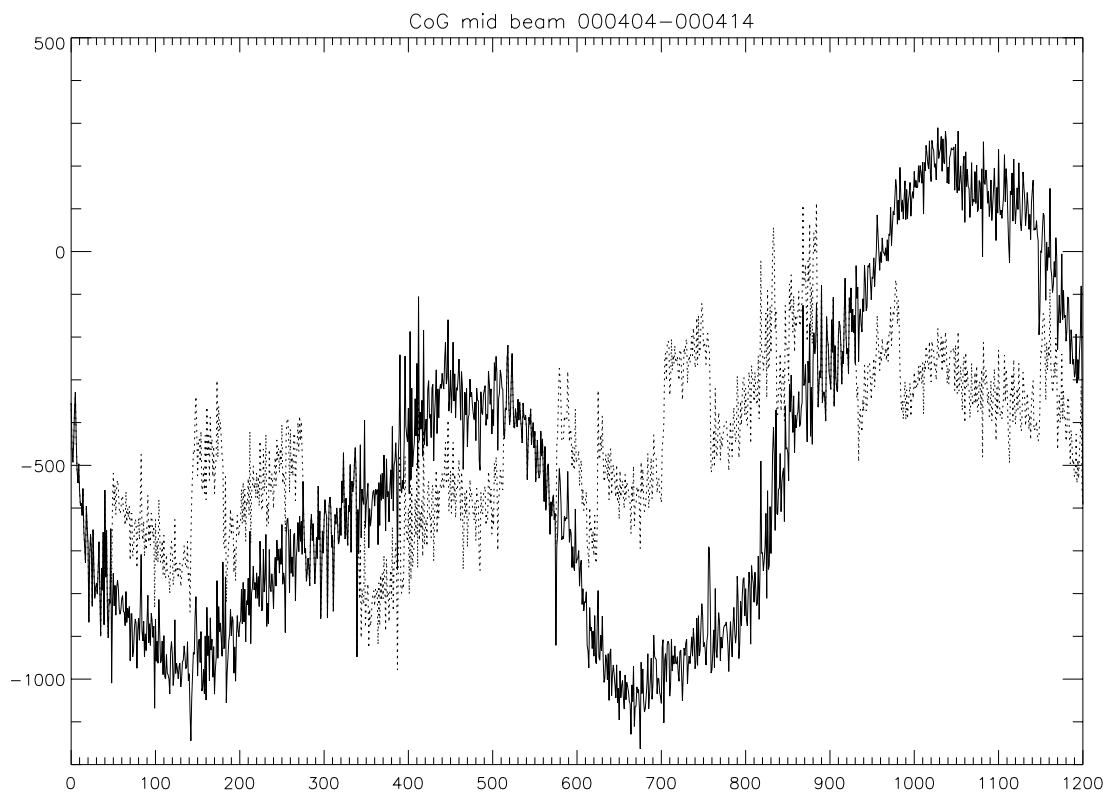


FIGURE 21. Evolution of the Mid beam CoG from Ascending node time (1 unit = 5 s.) gyro=5.Beginning of April 2000.

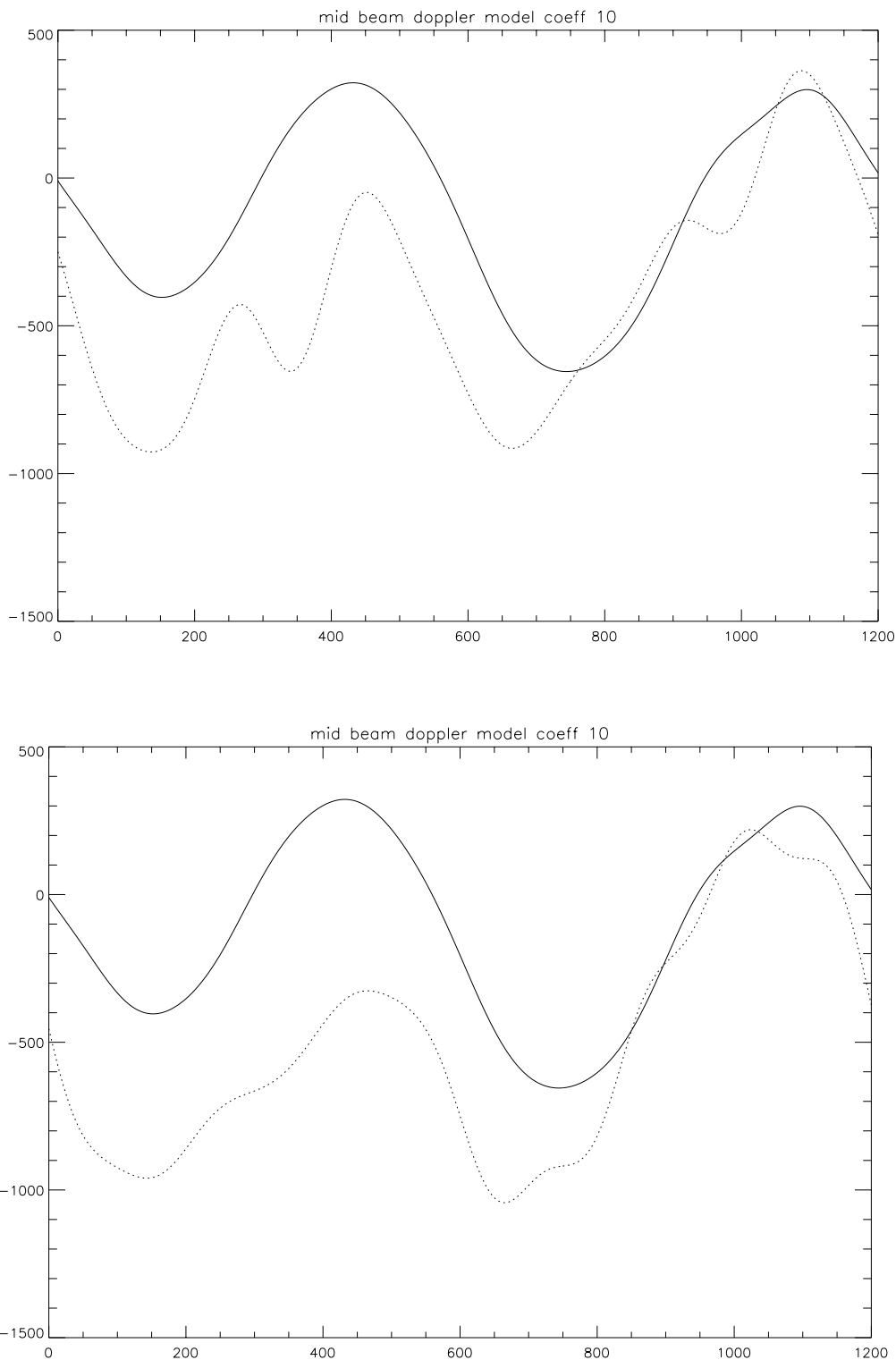


FIGURE 22. Comparison between the three gyro configuration (solid line) and mono gyro (gyro=5) configuration. Low pass filtered evolution of the Mid beam CoG from Ascending node (1 unit = 5 s.). Upper plot is during the qualification period (mid February 2000). Lower plot is at the beginning of April 2000.

3.2 Noise power level I and Q channel

The results of the monitoring are shown in Figure 23. The first set of three plots presents the noise power evolution for the I channel while the second set shows the Q channel. The noise level is less than 1 ADC Unit for the fore and aft signals and is negligible for the mid one. From the plots one can see that the noise level is more stable in the I channel than in the Q one. The PCS suspects that an explanation should be found in the different position of the receivers, in particular it seems that the Q one is closer to the ATSR-GOME electronics. A confirmation of this hypothesis has been asked to ESTEC.

Since 5th December 1997 some high peaks appear in the plots. These high values for the daily mean are due to the presence for these special days of a single UWI product with an unrealistic value in the noise power field of its Specific Product Header. The analysis of the raw data used to generate these products lead in all cases to the presence of one source packet with a corrupted value in the noise field stored into the source packet Secondary Header. Table 4 presents the list of the UWI products affected by a corrupted noise field and disseminated during cycle 51.

Table 4: UWI products with noise field corrupted (cycle 51)

Noise Field corrupted	Noise value (ADC Unit)	Acquisition Time
None	-	-

The reason why noise field corruption is beginning from 5th December 1997 is at present unknown. It is interesting to note that at the beginning of December 1997, we started to get as well the corruption of the Satellite Binary Times (SBTs) stored in the EWIC product. The impact in the fast delivery products was the production of blank products starting from the corrupted EWIC until the end of the scheduled stop time. A change in the ground station processing in March 1998 overcame this problem.

Since 9th August 1998 some periods with a clear instability in the noise power have been recognised. Table 5 gives the detailed list.

Table 5: ERS-2 Scatterometer instability in the noise power

From	To
9 th August 1998	26 th October 1998
29 th November 1998	6 th December 1998
23 rd December 1998	24 th December 1998
7 th June 1999	10 th June 1999
17 th August 1999	22 nd August 1999
8 th September 1999	9 th September 1999
3 rd October 1999	8 th October 1999
16 th October 1999	18 th October 1999
26 th October 1999	28 th October 1999

From	To
25 th December 1999	2 nd January 2000
10 th February 2000	11 th February 2000
19 th March 2000	26 th March 2000

To better understand the instability of the noise power the PCS has carried out investigations in the scatterometer raw data (EWIC) to compute the noise power with more resolution. The result is that for the orbits affected by the instability the noise power had a decrease of roughly 0.7 dB for the fore and aft signals and a decrease of roughly 0.6 dB in the mid beam case (see report cycle 42). The decrease of the noise power during the orbits affected by the instability is comparable with the decrease of the internal calibration level that occurred during the same orbits. The reason of this instability (linked to the AMI anomalies) is still under investigation. A plot that shows the correlation among the noise power, the internal calibration level and the AMI anomaly is reported in section 3.3.

Figure 24 shows the evolution of the noise power since 26th October when 2 dB were added to the transmitted power. The periods with the instability in the noise are clear shown in the plots, in particular for the channel I plots (fore and aft beam).

During cycle51 the evolution of the noise power was stable apart from the period 19th - 26th March when three AMI anomalies caused an instability in the noise power and in the internal calibration level.

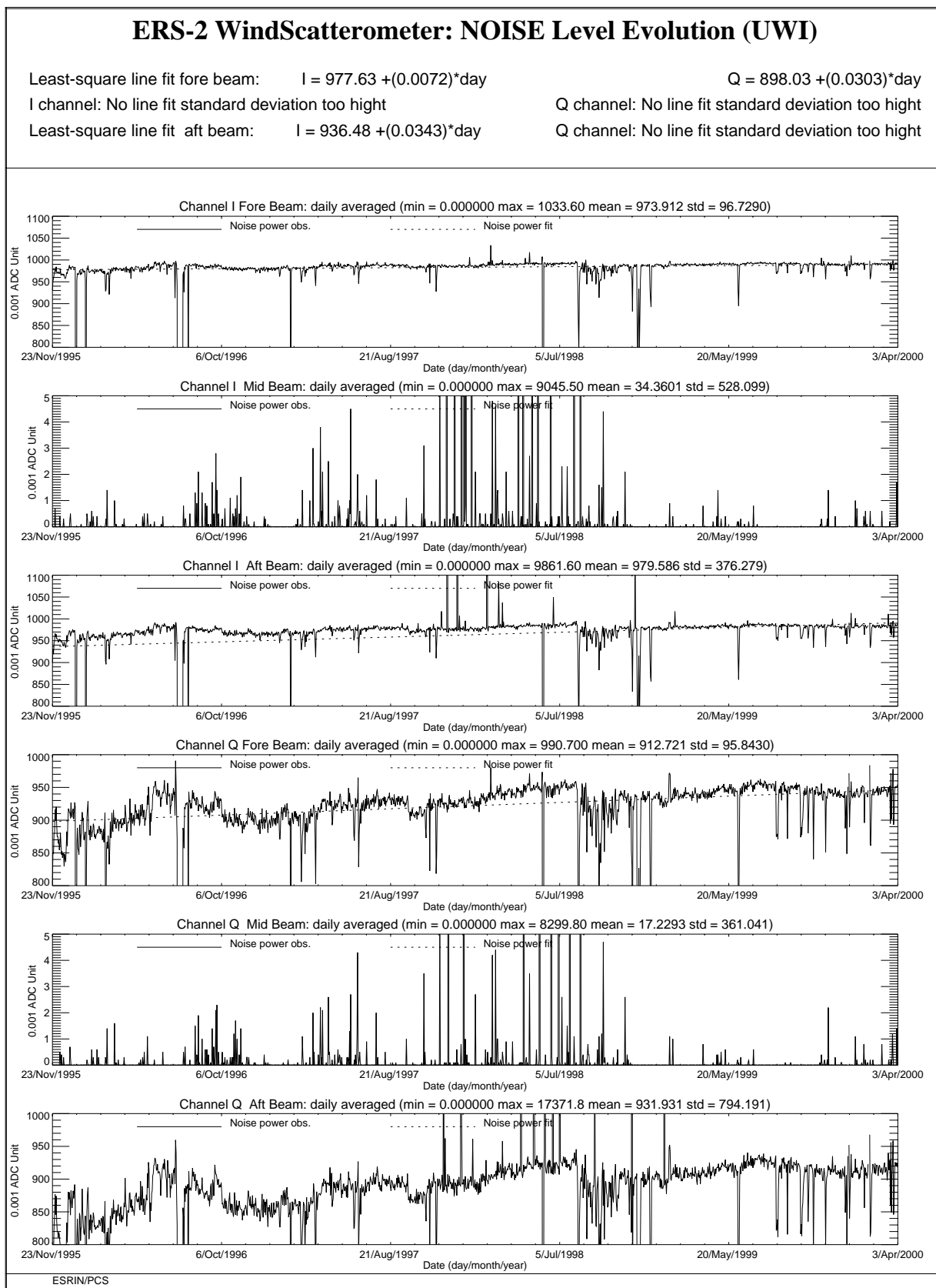


FIGURE 23. ERS-2 Scatterometer: noise power I and Q channel since the beginning of the mission.

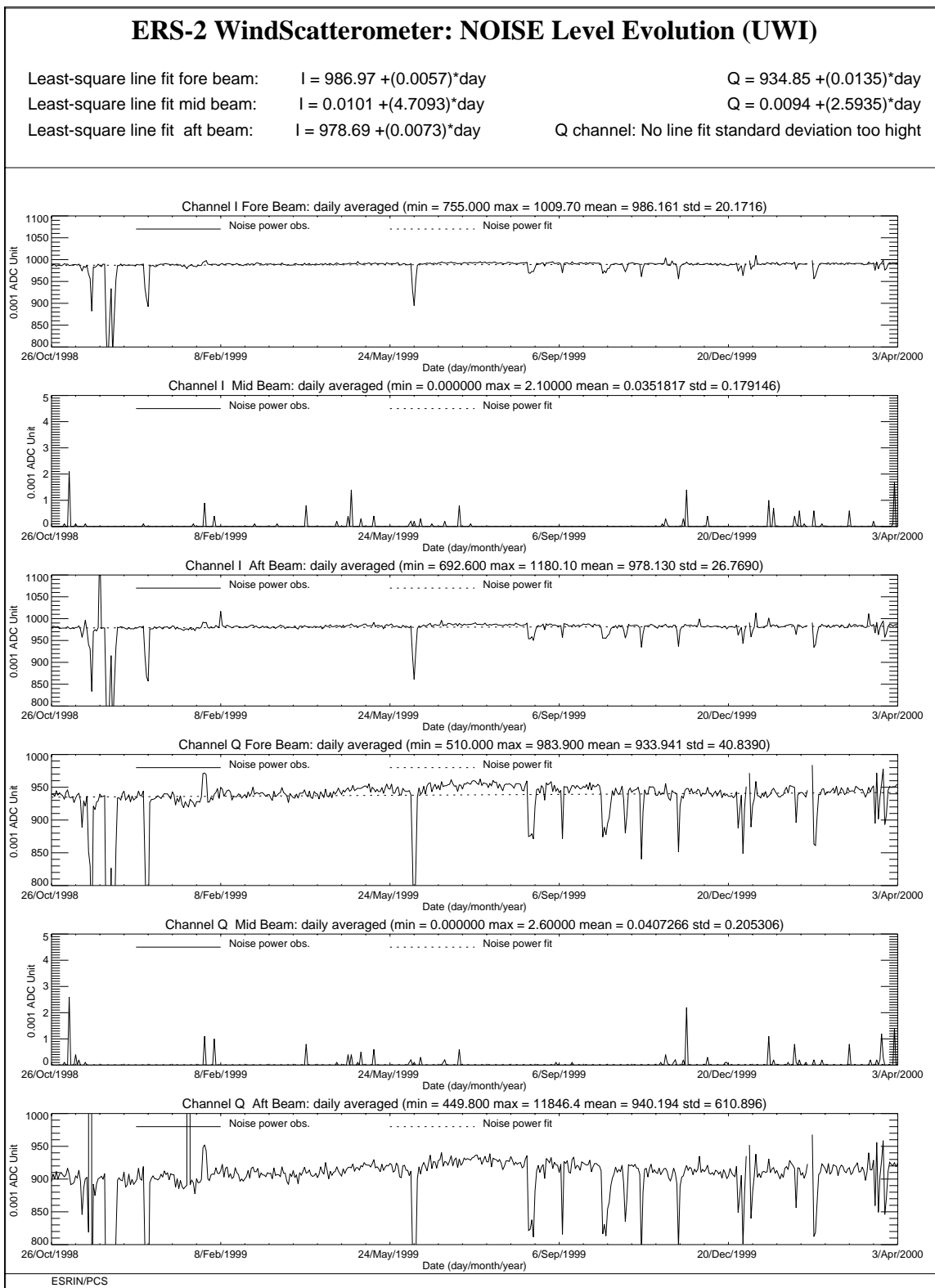


FIGURE 24. ERS-2 Scatterometer: noise power I and Q channel since 26th October 1998 when the transmitted power was increased by 2 dB.

3.3 Power level of internal calibration pulse

For the internal calibration level, the results, since the beginning of the mission, are shown in Figure 26.

The high value of the variance in the fore beam until August, 12th 1996 is due to the ground processing. In fact all the blank source packets ingested by the processor were recognized as fore beam source packets with a default value for the internal calibration level. The default value was applicable for ERS-1 and therefore was not appropriate for ERS-2 data processing. On August 12th, 1996 a change in the ground processing LUT overcame the problem.

Since the beginning of the mission a power decrease is detected. The reason is that the TWT is not working in saturation, so that a variation in the input signal is visible in the output. The variability of the input signal can be two-fold: the evolution of the pulse generator or the tendency of the switches between the pulse generator and the TWT to reset themselves into a nominal position. These switches were set into an intermediate position in order to put into operation the scatterometer instrument (on 16th November 1995). The power decrease is regular and affects the AMI when it is working in wind-only mode, wind/wave mode and image mode indifferently.

The power decrease is estimated to be about 0.0025 dB per day. After the change of the calibration subsystem on August 6th, 1996 the decrease is more evident and it is estimated in 0.09 dB per cycle.

On 26th October 1998 (cycle 37) to compensate for this decrease, 2.0 dB were added to the Scatterometer transmitted power and this explains the large step shows in Figure 25 and Figure 26. After that day the power decrease is on average 0.07 dB per cycle.

It is important to point out the efficiency of the internal calibration for keeping the absolute calibration level stable. In fact, no important change is noted in the monitoring of the gamma-nought level over the Brazilian rain forest during the power decrease and after the increase of the transmitted power (see section 2.0).

Since 9th August 1998 the internal calibration level shows an instability. This instability is very well correlated with the fluctuations observed in the noise power as outlined in section 3.2.

Figure 25 shows the daily average of the internal calibration and the noise power from 1st August 1998 to 4th April 2000. In the figure are also reported the anomalies that affected the AMI (the triangles in the plot) and the days when the instability was very strong (asterisks in the plot).

From Figure 25 it seems that there is a clear correlation between the instability (noise and calibration level) and the AMI anomalies.

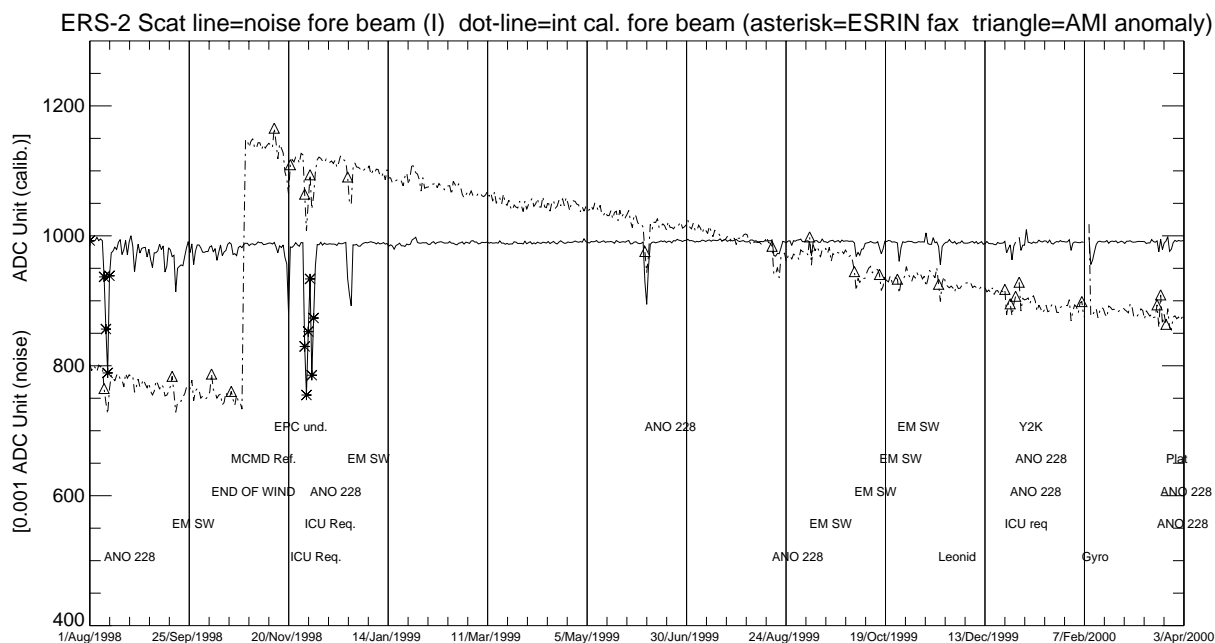


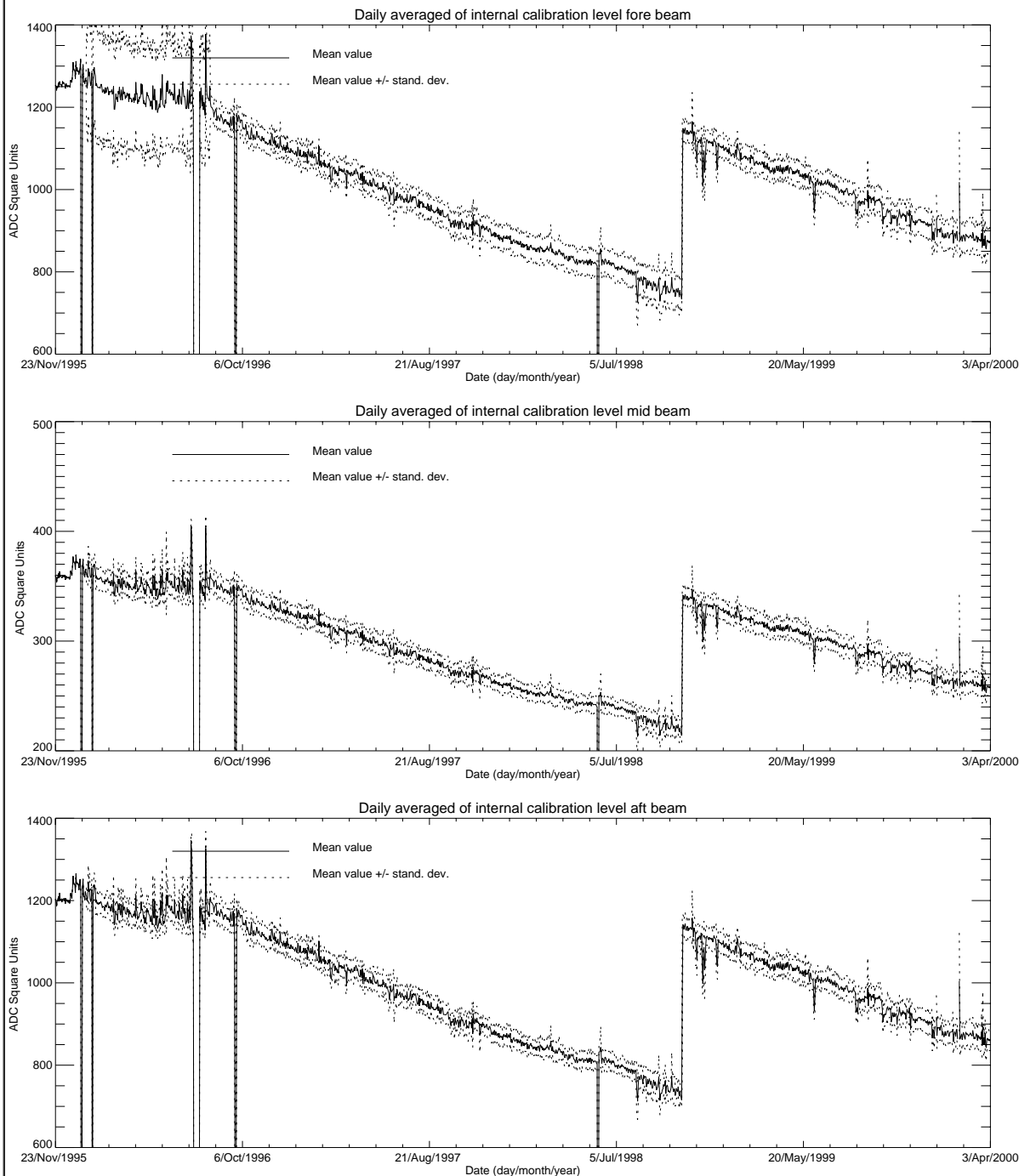
FIGURE 25. ERS-2 Scatterometer: noise power (I channel fore antenna) and internal calibration power (fore antenna) evolution from 1st August 1998 to 3rd March 2000.

During the cycle 51 the internal calibration level had, on average, a power decrease of 0.09 dB. This value is greater than the one computed for the previous cycle and it is due to the instability in the calibration level occurred after the AMI anomalies (see Figure 25).

Apart from the AMI anomalies the power decrease since 26th October 1998 is regular and it is on average 0.07 dB per cycle as shown in Figure 27.

ERS-2 WindScatterometer: Internal CALIBRATION Level Evolution (UWI)

Least-square polynomial fit fore beam	gain (dB) per day -0.0001	$1028.79 + (-0.0301381) \cdot \text{day}$
Least-square polynomial fit mid beam	gain (dB) per day -0.0001	$301.500 + (-0.00686100) \cdot \text{day}$
Least-square polynomial fit aft beam	gain (dB) per day -0.0001	$1009.91 + (-0.0258053) \cdot \text{day}$



ESRIN/PCS

FIGURE 26. ERS-2 Scatterometer: power of internal calibration pulse since the beginning of the mission.

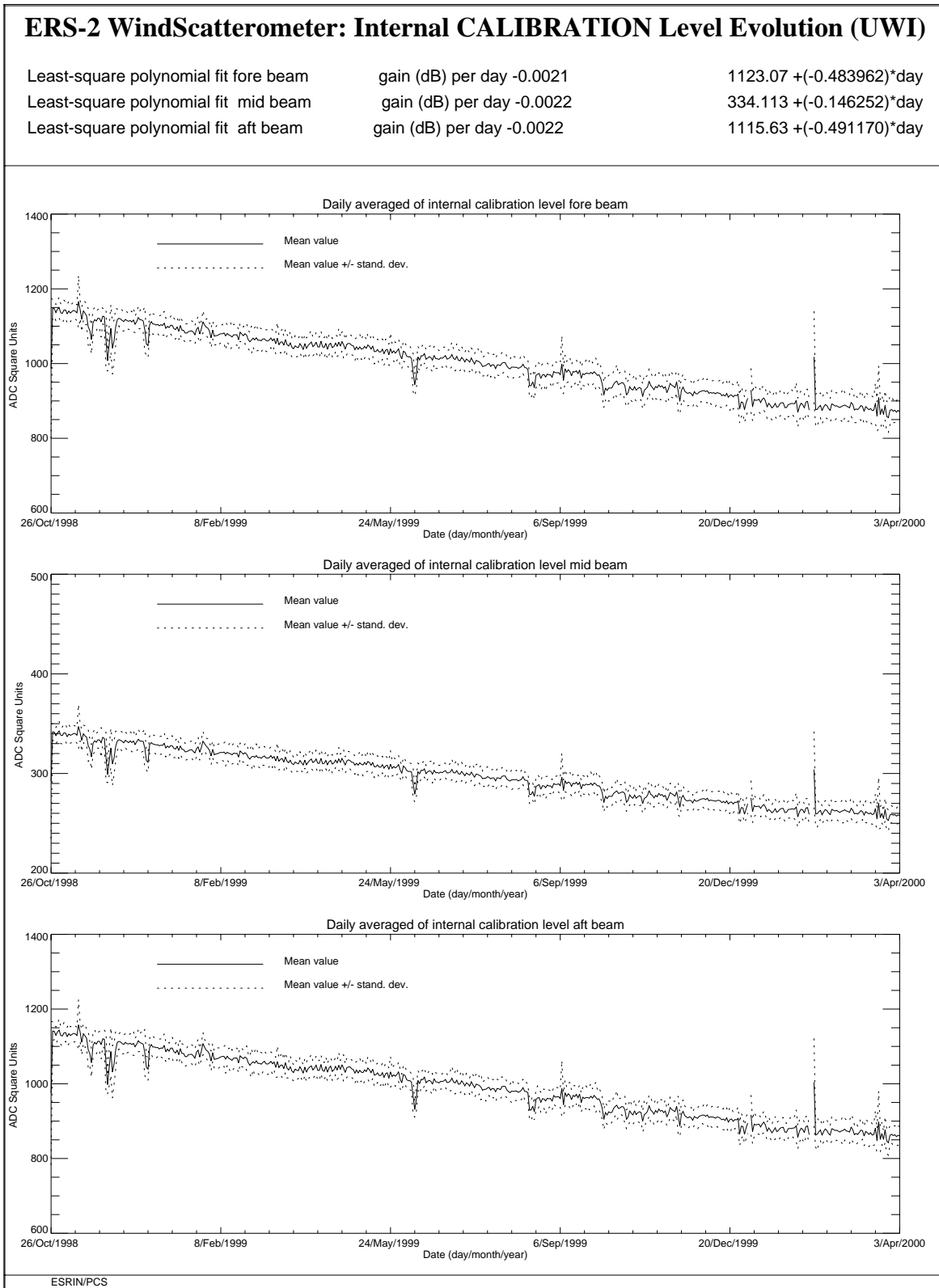


FIGURE 27. ERS-2 Scatterometer: power of internal calibration level since 26th October 1998 when the transmitted power was increased by 2.0 dB.

4.0 Products performance

One of the most important point in the monitoring of the products performance is their availability. The Scatterometer is a part of ERS payload and it is combined with a Synthetic Aperture Radar (SAR) into a single Active Microwave Instrument (AMI). The SAR users requirements and the constraints imposed by the on-board hardware (e.g. amount of data that can be recorded in the on-board tape) set rules in the mission operation plan.

The principal rules that affected the Scatterometer instruments are:

- over the Ocean the AMI is in wind/wave mode (scatterometer with small SAR imagerettes acquired every 30 sec.) and the ATSR-2 is in low rate data mode.
- over the Land the AMI is in wind only mode (only scatterometer) and the ATSR-2 is in high rate mode. (Due to on board recorder capacity, ATSR-2 in high rate is not compatible with Sar wave imagerette acquisitions.)

This strategy preserves the Ocean mission.

Moreover:

- the SAR images are planned as consequence of users' request.

These rules have an impact on the Scatterometer data availability as shown in Figure 28.

Each segment of the orbit has different colour depending on the instrument mode: brown for wind only mode, blue for wind-wave mode and green for image mode. The red and yellow colours correspond to gap modes (no data acquired). The major problems came from the orbit segments between Australia and Antarctic and between Africa and Antarctic where a lot of data are not acquired. This problem is under investigation by ESRIN and a new mission operation plan for the scatterometer shall be adopted.

For cycle 51 the percentage of the ERS-2 AMI activity is shown in table 6.

Table 6: ERS-2 AMI activity (cycle 51)

AMI modes	ascending passes	descending passes
Wind and Wind-Wave	87.4%	81.5%
Image	2.4%	7.0%
Gap and others	10.2%	11.5%

The percentage of scatterometer activity during the cycle 51 was within the nominal value.

Table 7 reports the major data lost due to the test periods and AMI or satellite anomalies occurred after August 6th, 1996 (before that day for many times data were not acquired due to the DC converter failure).

Table 7: ERS-2 Scatterometer mission major data lost after 6th, August 1996

From	To	Reason
September 23 rd , 1996	September 26 th , 1996	ERS-2 switched off due to a test period
February 14 th , 1997	February 15 th , 1997	ERS-2 switched off due to a depointing anomaly
June 3 rd , 1998	June 6 th , 1998	ERS-2 switched off due to a depointing anomaly
November 17 th , 1998	November 18 th , 1998	ERS-2 switched off to face out Leonide meteo storm
September 22 nd , 1999	September 23 rd , 1999	ERS-2 switched off due to Year 2000 certification test
November 17 th , 1999	November 18 th , 1999	ERS-2 switched off to face out Leonide meteo storm
December 31 st , 1999	January 2 nd , 2000	ERS-2 switched off Y2K transition operation
February 7 th , 2000	February 9 th , 2000	ERS-2 switched off due to new AOCS s/w up-link

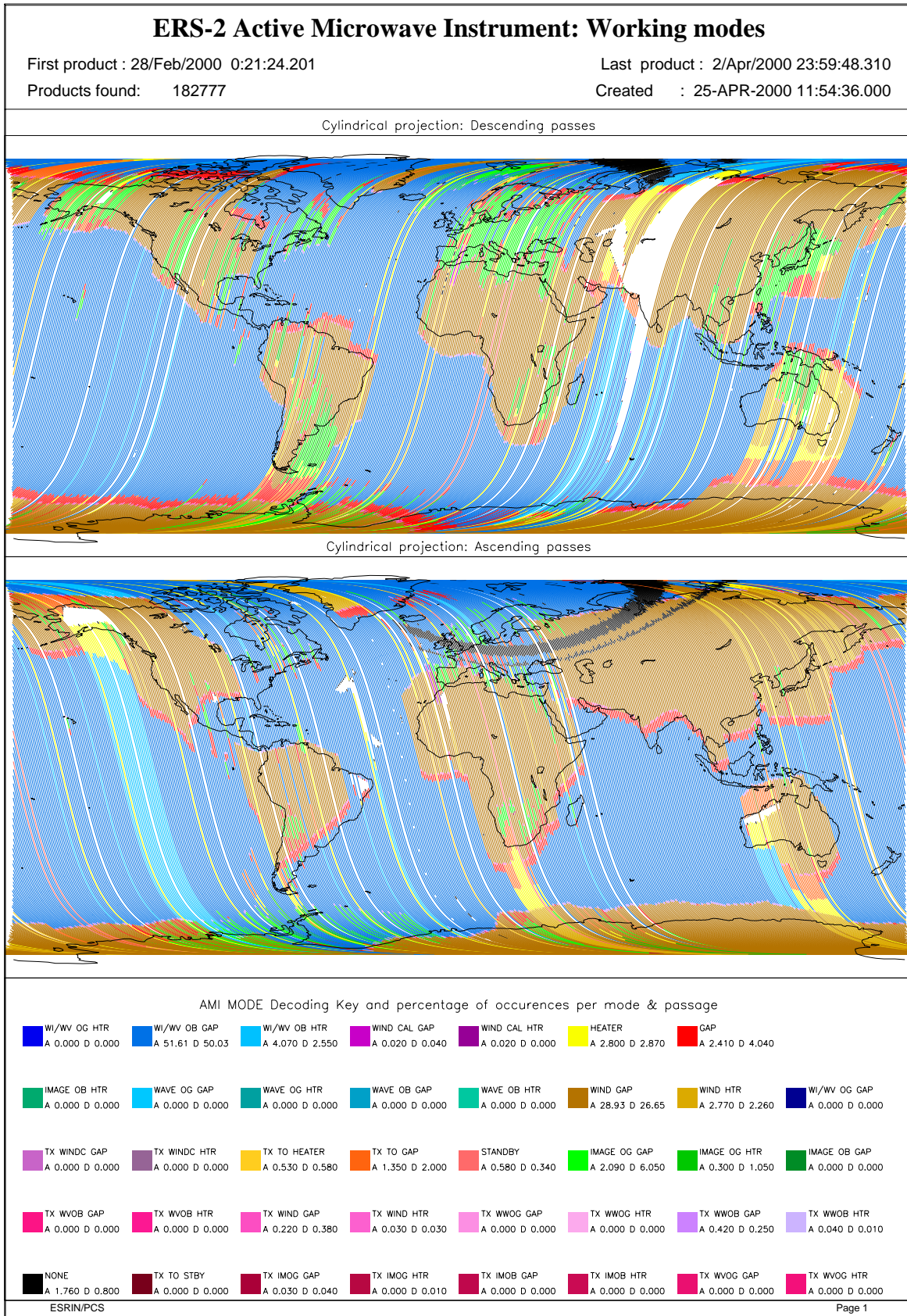


FIGURE 28. ERS-2 AMI activity during cycle 51.

The PCS carries out a quality control of the winds generated from the WSCATT data. The activity is split in two main areas: the first one includes a routine analysis of the fast Delivery Products disseminated to the users, the second one is focused on the improvement of the CMOD-4 (the operative ESA wind retrieval algorithm) for high wind speed (for more information see on the Web site <http://pcswwww.esrin.esa.it> the Cyclone Tracking home page). External contributions to this quality control come also from ECMWF and UK-Met Office.

The routine analysis is summarized in the plots of figure 29; from top to bottom:

- the monitoring of the valid sigma-nought triplets per day.
- the evolution of the wind direction quality. The ERS wind direction (for all nodes and only for those nodes where the ambiguity removal has worked properly) is compared with the ECMWF forecast. The plot shows the percentage of nodes for which the difference falls in the range -90.0, +90.0 degrees.
- the monitoring of the percentage of nodes whose ambiguity removal works successfully.
- the comparison of the wind speed deviation: (bias and standard deviation) with the ECMWF forecast.

The results since the beginning of the mission can be summarized (after August 6th, 1996 and apart from the events given in Table 7) as:

- a stable number of valid sigma-nought with a small increase after June 29th, 1999 due to the dissemination in fast delivery of the data acquired in the Prince Albert station.
- an accurate wind direction for roughly 93% of the nodes, a success in the ambiguity removal for more than 90.0% of the nodes.

The ERS-2 wind speed shows an absolute bias of roughly 0.5 m/s and a standard deviation that ranges from 2.5 m/s to 3.5 m/s with respect to the ECMWF forecast. The wind speed bias and its standard deviation have a seasonal pattern due to the different winds distribution between the winter and summer season.

It is important to note that only after the end of calibration phase (mid March 1996) the wind products have reached high quality.

Two important changes affect the speed bias plot: the first is on June 3rd, 1996 and it is due to the switch from ERS-1 to ERS-2 data assimilation in the meteorological model. The second change, which occurred at the beginning of September 1997, is due to the new monitoring and assimilation scheme in ECMWF algorithms (4D-Var).

Since 19th April 1999 two set of meteo-table (meteorological forecast centred at 00:00 and 12:00 of each day) are used in the ground processing. With this new strategy the data are processed using the 18 and 24 hours meteorological forecast instead of the 18, 24, 30 36 hours forecast. The data processed with the 18-24 hours tables instead of 30-36 hours tables have an increase in the number of ambiguity removed nodes but no important improvements are shown, on average, in the daily statistics.

Since 25th August 1999 a new LRDPF software (version 8500) is operative in the ground stations. With this upgrade the LRDPF is year 2000 compatible; no changes were introduced in the scatterometer data processing.

The new AOCS configuration (see report for cycle 50) that is operative since 7th February 2000, did not affect the wind data performance.

For cycle 51 the PCS quality control has reported stable results.

The number of valid triplets acquired per day was stable around 180000 (apart from days 19th, 21th, 24th and 25th March 2000 when the number of valid triplets was less than the nominal value. This because the AMI instrument was unavailable for some orbits).

The wind speed bias (UWI -ECMWF Forecast) was close to 0 m/s and the wind speed standard deviation was between 2.5 m/s and 3.0 m/s. The ambiguity removal rate was working fine for more than 90% of nodes.

The ECMWF (see annex) reports a wind speed bias (UWI-FG) of -0.76 m/s with a standard deviation of 1.55 m/s. The comparison between FG and 4D-var shows a wind speed bias of -0.48 with a standard deviation of 1.63 m/s. The directional bias is close to zero for both the products. These results are very similar to the ones of the last monitoring report.

.

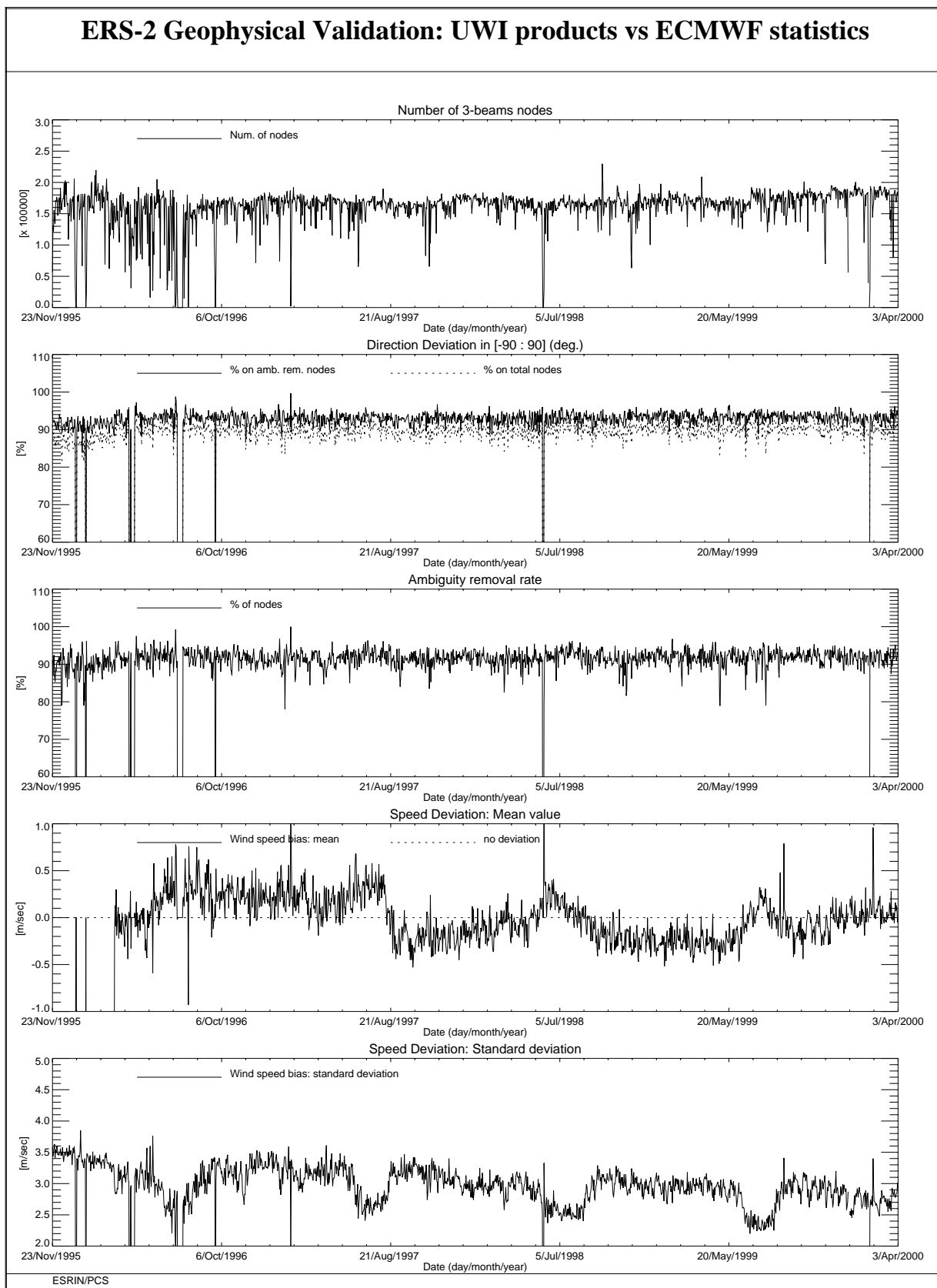


FIGURE 29. ERS-2 Scatterometer: wind products performance since the beginning of the mission.

